

# Macroscopic condensation of photon noise in sharply nonlinear dissipative systems

Nicholas Rivera<sup>1</sup>, Jamison Sloan<sup>2</sup>, Yannick Salamin<sup>2</sup>, and Marin Soljačić<sup>1,2</sup>

<sup>1</sup>*Department of Physics, MIT, Cambridge, MA 02139, USA.*

<sup>2</sup>*Research Laboratory of Electronics, MIT, Cambridge, MA 02139, USA.*

## Abstract

Macroscopic non-Gaussian states of light are among the most highly-coveted “holy grails” in quantum science and technology. An important example is that of macroscopic number (Fock) states of light. Due to their exactly defined number of photons, they are of great interest in quantum metrology, spectroscopy, simulation, and information processing. However, the deterministic creation and stabilization of even approximate large-number Fock states remains thus far a long-standing open problem. Here, we introduce a mechanism that deterministically generates macroscopic sub-Poissonian states, including Fock states, at optical and infrared frequencies. The method takes advantage of the fact that a photon with a sharply increasing nonlinear loss will have its intensity noise condense as it decays. We reveal regimes where this phenomenon can lead to transient generation of Fock and sub-Poissonian states. We further show that these low noise states can be preserved in steady-state by building a laser with a sharp loss element, stabilizing the state with an equilibrium between gain and loss. We show two examples of these phenomena: one which produces a near-Fock state with 5,000 photons (with an uncertainty of  $< 1$  photon), and one which generates a macroscopic sub-Poissonian state with  $10^{12}$  photons, yet noise 99% below that of a coherent state of the same size. When realized, our results may enable many of the previously envisaged applications of number states and sub-Poissonian states for quantum algorithms, simulation, metrology, and spectroscopy. More generally, our results provide a new and general type of nonlinearity which could form the basis for many new optoelectronic devices which emit macroscopic non-Gaussian light.

Light is among the most important tools by which we understand and control the physical world. It enables precise measurements of physical properties, preparation and probing of desired states of matter, and efficient long-distance communication. Our capabilities are further enriched by exploiting the quantum nature of light, bringing these applications beyond the limits ostensibly imposed by classical physics. Much of the current focus is on the use of quantum states of light such as single-photons, entangled photon pairs, cluster states, and quadrature-squeezed light [1–6].

While already useful for some applications, a complete transformation of the quantum landscape is expected if macroscopic non-Gaussian states of light, which offer the most unique degree of quantum advantage, could be deterministically realized. As one concrete example, consider what would happen if one could realize an extremely nonclassical state, such as a large Fock state of light. Such states have long been eyed in quantum metrology because they have a perfectly defined intensity that would enable measurements without shot noise [7–9]. However, the largest optical Fock state realized so far has just two photons, limiting the attainable benefit in applications. Perhaps one of the highest-profile applications of large Fock states would be for a quantum algorithm such as boson sampling (or gaussian boson sampling) [10–15]: a “modest” (multimode) Fock state of even 100 photons enables computations of matrix permanents at least fifteen orders of magnitude larger than could be handled by even the largest supercomputers today [16], and would resoundingly bring the promise of quantum computation to reality. Perhaps from a more fundamental perspective, the realization of a large Fock state would constitute a new macroscopic manifestation of quantum mechanics, not totally dissimilar to effects like superconductivity and Bose-Einstein condensation. Such macroscopic nonclassical light could be used to drive nonlinear dynamics in atoms, molecules, and solids, giving birth to many new quantum nonlinear phenomena.

Despite the potential rewards, deterministic generation of large Fock states remains an open problem. Part of the reason is that no generic interactions between light and matter naturally select for large- $n$  Fock states. This is in contrast to, say, Gaussian states like coherent states and squeezed states, which can be macroscopically produced by means of lasers or nonlinear media [17]. The other key issue is that Fock states are fragile and destabilize in the presence of dissipation [18]. Loss introduces photon number uncertainty into a Fock state, as photon absorption is probabilistic.

Due to these challenges, the approach that has led to record Fock states (about 15 microwave photons) is based on transient accumulation of photons in a cavity at precise times using cavity quantum electrodynamical interactions with superconducting qubits, as demonstrated in [18, 19].

Fock states generated this way could then be used as a resource state to simulate vibronic spectra of molecules [20]. It is important in these techniques that the photons are built up before losses set in, setting the maximal Fock state that is generated. Other exciting schemes applied at microwave frequencies include the “micromaser” [17, 21, 22] and quantum feedback protocols [23]. Such techniques cannot at present be extended to optics: thus, generating Fock states of even two or more photons is difficult (one-photon states are generated by quantum emitters and also by heralding photon pairs produced by parametric down-conversion). Fock states can also be non-deterministically generated by collapsing the wavefunction in the number basis [24, 25] or via quantum non-demolition measurement [26].

Here, we introduce schemes to produce close approximations to high photon-number optical Fock states. Our proposals leverage existing systems to produce low-noise states of light with photon numbers orders of magnitude above what has been realized, or even predicted. Central to these schemes is a new type of nonlinearity that we identify (and show how to construct) which naturally produces Fock states [67]. In particular, we show the presence of sharply intensity-dependent dissipation is key. When engineered appropriately, intensity-dependent loss can create a trapping potential for the photon in the number space, strongly favoring low-noise states.

In principle, this mechanism can produce exact Fock states (under conditions we discuss). In practice, various factors which we take into account will lead to very close approximations to Fock states, but states with far lower noise than realized, which should prove beneficial for many applications above. In cases where Fock states are not produced, the method can produce macroscopic light with intensity noise far below the shot-noise limit. For example, we show how states with 5000 photons can be realized with an uncertainty of just one photon. For example, we show how it may be possible to produce macroscopic states of a cavity resonator with intensity noise nearly 99% below the shot noise limit, yet with  $10^{12}$  photons in the resonator (corresponding to intracavity optical powers of 10 W). We show how these concepts can apply to transient schemes, as well as steady-state schemes. In the transient case, we show how a freely decaying field in a resonator can compress its noise as it decays, as a result of suitably engineered nonlinear loss. In the steady-state case, we show how to stabilize such low noise states by building a fundamentally new type of laser in which these nonlinear losses (rather than saturable gain) provide the saturation mechanism: here, the low noise state is stabilized by the equilibrium between gain and loss (e.g., using the laser principle). We also discuss the relation to prior art, paths to experimental realization (and important experimental considerations), as well as exciting research directions that follow from

our results.

The text is organized as follows: we present the main results of our theory of nonlinear dissipative processes in quantum optics. We use it to construct classes of nonlinear dissipation that enable the generation of low-noise and even Fock states. In Sec. II, we use these results to “transiently” produce such states. They will not be stable against residual linear dissipation that is always present. However, we then show how to stabilize such low-noise states by suitably introducing a gain medium in Sec. III. In the manuscript, we stick to discussing the effect in terms of “intuition” and relatively simple equations. In Sections II and III, we introduce example systems using parameters corresponding to existing systems (nascent and mature) to show that this effect is within reach of current technology. The purpose of these examples is to demonstrate the types of systems which could realize the effects developed here.

We should strongly emphasize that all of the presented equations and results follow from a rigorous quantum optical theory of dissipation of anharmonic oscillators coupled to a frequency-dependent dissipation channel. We derive these results in the SI, through a density matrix, as well as a Heisenberg-Langevin approach (the results are in exact agreement). Thus, one may argue that the main theoretical contribution of this work is the identification of a class of Liouvillians that either transiently (under certain initial conditions), or in steady-state, produce Fock states and close (highly sub-Poissonian) approximations of them. The other main contribution of this work is identification of candidate systems to realize these effects. The scope of systems covered by our theory is far larger than these particular examples and implementations.

## **I. SPONTANEOUS NOISE CONDENSATION IN SYSTEMS WITH SHARPLY INTENSITY-DEPENDENT LOSS**

In this section, we introduce a type of nonlinear optical loss which causes the photon number noise of a photonic state to spontaneously condense. Then we introduce a class of systems that realizes the desired nonlinear loss. The systems combine conservative Kerr nonlinearities with frequency-dependent (dispersive) losses, to create a loss with an effectively non-perturbative intensity dependence (in contrast to low-order nonlinearities like second- and third-order ones) [68]. In the Methods section, we develop a general quantum-optical theory of dissipation in an anharmonic oscillator coupled to frequency-dependent losses, exemplifying it with a model that is rigorously shown to meet the requirements for noise condensation. Derivations, as well as further

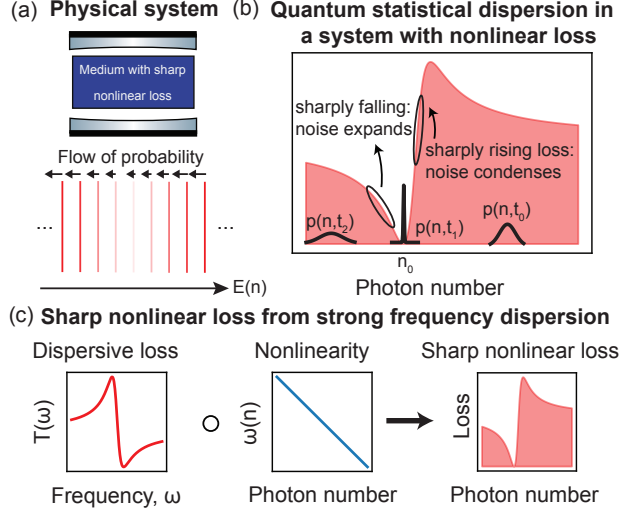


**FIG. 1: Photon noise condensation in systems with sharply nonlinear loss, as realized by an anharmonic oscillator with sharply frequency-dependent loss.** (a) The physical system under consideration is a single-mode (or effectively single-mode) optical resonator with a sharply intensity-dependent nonlinear loss. The sharp loss can be understood as affecting the flow of probabilities between neighboring Fock states of the anharmonic oscillator. (b) Quantum dispersion of photon probabilities in the presence of sharp loss. An initial probability distribution  $p(n, t_0)$ , as it moves to lower photon numbers due to losses, will expand when it moves through a region of falling losses (noise increases), and condense as it moves through a region of increasing losses (noise decreases). Note that  $t_0 < t_1 < t_2$ . (c) Realizing the sharp loss of (b) may be accomplished by taking a system with a sharply frequency-dependent transmission or absorption (as in the first panel of (c)) and integrating it into a resonator with a Kerr nonlinear medium into it. The frequency-dependent loss and the number-dependent frequency “compose” to create the desired intensity-dependent loss.

evidence supporting the model we introduce, are shown in the Supplementary Information (SI).

In this work, we will focus on the quantum dynamics of the electromagnetic field in a single-mode optical cavity. In the discussion, we will say more about Fock states of freely propagating photons. Consider a resonator with dissipation (depicted in Fig. 1(a)). For our purposes, we will generally consider dissipation that results from radiative leakage, but it may also arise from suitably engineered internal cavity losses [69]. The dissipation can be described in terms of quantum transitions from the  $n$ -photon state of the cavity to the  $n - 1$  state, causing the probability of the  $n$ -photon state  $p(n)$  to decrease. The rate of the transition  $n \rightarrow (n - 1)$  is defined as  $L(n)$ . There

is also a flow of probability into the  $n$ -photon state arising from the transition  $(n + 1) \rightarrow n$  at rate  $L(n + 1)$  (probability flows are schematically depicted in Fig. 1(a)). In this case, the rate of change of the probability distribution of the cavity photon takes the form:

$$\dot{p}(n) = -L(n)p(n) + L(n + 1)p(n + 1). \quad (1)$$

The most common case of this equation is that of linear loss, in which  $L(n) = \kappa n$ , where the (temporal) decay rate  $\kappa$  of the photon is independent of photon number [27]. In this work, we will be interested in nonlinear loss, which is expressed by  $L(n) = \kappa(n)n$ .

We now describe the dynamics of light subject to the rate equation of Eq. 1. While the solution to this rate equation contains all of the statistical properties of the photon probability distribution, the distribution is most conveniently understood through its first two cumulants (the mean and variance). A variance  $(\Delta n)^2 = 0$  indicates a Fock state. Supposing that the uncertainty  $\Delta n \ll n$ , which is almost universally the case for macroscopic light, the mean  $\bar{n}$  and variance  $(\Delta n)^2$  evolve according to the equations (see SI for derivation):

$$\begin{aligned} \dot{\bar{n}} &= -L(\bar{n}) \\ (\dot{\Delta n})^2 &= L(\bar{n}) - 2L'(\bar{n})(\Delta n)^2. \end{aligned} \quad (2)$$

Note that by  $L'(\bar{n})$ , we mean  $\left. \frac{dL}{dn} \right|_{\bar{n}}$ . Consider first the case of coherent light decaying by means of linear loss ( $L(\bar{n}) = \kappa \bar{n}$ ). At time zero  $(\Delta n)^2 = \bar{n}$ , and therefore  $\dot{\bar{n}} = (\dot{\Delta n})^2$ , implying that at all times, the photon remains coherent. Now, we consider the case in which coherent light decays by nonlinear loss. If  $L'(\bar{n})(\Delta n)^2 > L(\bar{n})$  (which, for a coherent state, implies  $\bar{n}L'(\bar{n}) > L(\bar{n})$ ), then the variance will decay faster than the mean, leading to light with noise lower than that of a coherent state ( $(\Delta n)^2 < \bar{n}$ , also known as sub-Poissonian light [8] [70]). On the flip side, if the loss increases as the cavity field decays ( $L' < 0$ ), the photon noise will increase (potentially yielding super-Poissonian light). These two cases are illustrated in Fig. 1(b). In either case, the sharper the loss, the stronger the dispersion of the photon probability distribution. Another important observation concerns the case when  $L(\bar{n})$  contains a zero (at  $n_0$ ). In this case, photons entering the state  $n_0$  from above cannot leave. If  $L'(n_0^+) > 0$ , then the photon noise will be forced to condense indefinitely, approaching a Fock state of size  $n_0$ . In reality,  $L(\bar{n}) = 0$  is of course unattainable, as even if the nonlinear loss nearly vanishes, there will always be some other sources of small loss present. We will show that for background losses that are in principle achievable, very high degrees of noise condensation are attainable, even with macroscopic light.

To summarize the discussion of Eqs. (1, 2): a sharply increasing intensity-dependent loss lends itself to the production of Fock and sub-Poissonian states of light [71].

The observations of the previous paragraph lie at the core of this work. We now describe how a loss of this type may be realized. The basic idea is shown in Fig. 1(c): consider a system with a strong frequency-dependent loss (e.g., due to a frequency dependent transmission  $T(\omega)$  or a frequency-dependent absorption  $A(\omega)$ ). In a cavity with an intensity-dependent nonlinearity, the resonance frequency depends on the number of photons  $n$  in the cavity ( $\omega = \omega(n)$ ), as a result of the corresponding dependence of the effective refractive index on intensity. From a quantum mechanical perspective,  $\omega(n)$  corresponds to the frequency difference between states with  $n - 1$  and  $n$  photons. In other words, for a nonlinear system with a Kerr-type nonlinearity, such that  $H_a = \hbar\Omega(a^\dagger a)$ , one would say  $\omega(n) \equiv \omega_{n,n-1} = [\Omega(n) - \Omega(n - 1)]$ . For concreteness, we will consider the type of anharmonic Hamiltonian realized by a third-order nonlinear medium inserted into a cavity, with Hamiltonian  $H_a/\hbar = \omega (a^\dagger a + \beta(a^\dagger a)^2)$ . Here,  $\beta$  represents the dimensionless nonlinear strength associated with a single photon, so that the “frequency of a photon” depends on photon number as  $\omega(n) = \omega(1 + \beta + 2\beta n) \approx \omega(1 + 2\beta n)$  [28]. This equation expresses the familiar fact that in a resonator with a nonlinear element, the cavity frequency depends on the intracavity intensity through the corresponding dependence of the refractive index on intensity [29]. The loss will inherit a dependence on photon number (e.g.,  $T = T(\omega(n))$  or  $A = A(\omega(n))$ ), leading to a non-perturbative dependence of the dissipation on photon-number which can look like that of Fig. 1(b) (this kind of reasoning is important, for example, in the theory of optical bistability [30, 31]). The picture to have in mind is as follows: as light bounces around in the cavity, it will get dissipated by loss. As this happens, the intensity changes, and so does the resonance frequency of the cavity mode. The light will follow the instantaneous cavity mode and thus its frequency relative to that of the frequency-dependent loss element will change, thus changing its loss. In what follows, in the manuscript, we will consider the case of transmissive losses, which are more readily shaped in frequency, but these phenomena are also possible using absorption. The resulting loss, for a cavity of length  $L_c$  and a speed of light  $v$ , is given by

$$L(n) = n \frac{vT(\omega(n))}{2L_c}. \quad (3)$$

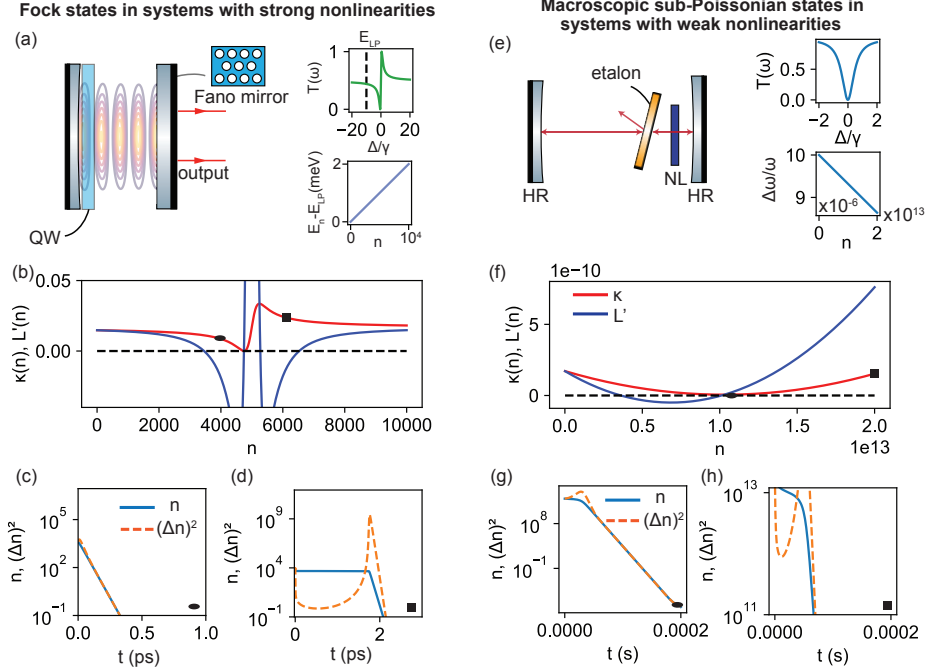


**FIG. 2: Transient noise condensation and production of Fock and macroscopic sub-Poissonian states of light.** (a) A system of excitons (in a quantum well (QW)) is strongly coupled to a resonant cavity in which one end-mirror is sharply frequency-dependent. The strong coupling of the excitons to the cavity leads to polaritons, which inherit a strong Kerr nonlinearity due to excitonic Coulomb interactions. (Inset) Transmission profile and nonlinearity of the lower polariton. The transmission is plotted in terms of the detuning  $\Delta$  of  $\omega$  from  $\omega_{\text{mirror}}$ . (b) Loss  $\kappa$  and its loss-derivative  $L'$  for the transmission profile shown in green and polaritons with Kerr nonlinear strength  $10^{-7}\omega_{\text{LP}}$ . The detuning of the mirror from the lower polariton energy (with zero polaritons) is  $10^{-3}\omega_0$  and the mirror has a sharpness of  $10^{-4}\omega_0$ . The black ellipse and square denote two different initial conditions for the photon probability distribution (in both cases, Poisson distributions with the mean indicated by the position of the ellipse and square). (c,d) Mean (blue) and variance (orange) of the photon number distribution for two different initial coherent states to the left and right of the approximate zero of  $\kappa$ . The state starting with lower photon number stays effectively coherent while the state with large coherent number has its noise condense to a value 1000-fold below the shot noise limit. (e-h) The same as above, except for a macroscopic optical (semi-confocal) cavity formed by two high-reflectivity (HR) mirrors, a nonlinear crystal (NL), and an etalon with a sharply varying transmission. In this case, initial states above the approximate zero of the transmission have their noise condensed 10-fold below the shot noise limit.



## II. CONVERSION OF COHERENT LIGHT INTO MACROSCOPIC SUB-POISSONIAN AND FOCK STATES OF LIGHT

With the model derived, we now show examples of how approximations to macroscopic Fock states can be transiently produced during the free decay of a coherent state in a resonator with nonlinear loss. We will show two examples: one in a “mesoscopic” regime, producing states with about 5,000 excitations, but with an uncertainty below 1 (effectively yielding a close approximation to a very large optical Fock state); and another in a “macroscopic” regime ( $n > 10^{12}$ ), in which the uncertainty is much greater than 1, but much less than  $\sqrt{n}$ , corresponding to non-classical light with sub-Poissonian statistics. The point of the former example is to show effectively a “true Fock state”. The point of the second example is to show how the same principle can be applied to macroscopic light to achieve extremely large suppressions of intensity fluctuations. To help anticipate the choice of systems considered in this work, we note that we would like to optimize  $dL/dn \sim dT/dn = \frac{dT}{d\omega} \frac{d\omega}{dn} \sim \beta dT/d\omega$ . Thus, generally one wants a strong nonlinearity, as well as a sharp transmission (so small linewidth  $\gamma$  [72]).

With this in mind, the first system we consider is shown in Fig. 2(a). It consists of a quantum well in between two mirrors (e.g., Bragg mirrors). The exciton of the quantum well couples strongly to the cavity mode, forming exciton polariton excitations (a lower and upper polariton state; we focus on the lower polariton for concreteness). Remarkable recent work has shown that the polaritons inherit the strong excitonic nonlinearities arising from Coulomb interactions between excitons [32], effectively leading to very strongly interacting photons [33]. Thus, these systems realize a dissipative Kerr model [34]. The same works have also shown how such exciton polaritons can be pumped coherently just like pure photons in a cavity (e.g., the mathematical description is identical since they are photonic quasiparticles [35]), and display similar quantum optical phenomena to nonlinear photons such as antibunching and bistability. These exciton polariton states can thus be treated as photons with an effective nonlinearity, so are within the scope of our theory.

Let us consider the dynamics of a coherent state of exciton polaritons (for concreteness, the lower polariton) in a cavity for which one of the two mirrors is perfectly reflecting, and the other has a transmission profile given by the green curve in Fig. 2(a). The corresponding loss coefficient  $\kappa(n)$  and loss derivative  $dL/dn$  are shown in red and blue (Fig. 2(b)). The dynamics of the coherent state depends quite strongly on the initial value of the photon number in the cavity relative

to the approximate zero of the transmission at  $n_0 \approx 5000$  (the zero in this case is not exact, as we consider an additional background linear loss with a quality factor  $Q_{\text{bg}} = 2 \times 10^6$ ). For an initial photon number below  $n_0$  (as in the black ellipse), the dynamics of the mean and variance (see Fig. 2(c)) behave as typically expected: the photon number decays exponentially, and the variance remains approximately equal to the mean. However, for an initial photon number larger than  $n_0$  (as in the black square), the variance drops much faster than the mean, as predicted by Eq. (2) (Fig. 2(d)). The uncertainty reaches a minimum of  $\Delta n \approx 0.8$  before rapidly increasing, reaching a noise three orders of magnitude lower than the shot noise limit. Notably, the mean photon number remains nearly constant as the noise condenses: this is a manifestation of the effect illustrated in Figs. 1(a,b). The loss is sufficiently low that probability gets trapped in these states (until the background loss “kicks in”). Since the probability distribution is trapped in a region where  $ndL/dn > L$ , the noise continues to condense, even as the photon number hardly changes. Note that this effect depends significantly on the magnitude of the background loss (and thus presents one of the main factors that must be mitigated in an experimental realization). For a background loss an order of magnitude stronger, the noise increases by a factor of three, but still stays a factor of 500 below the classical shot noise limit. Meanwhile, for absolute zero background loss, this equation predicts a complete condensation of noise to zero uncertainty.

The second system that we consider is motivated by the desire to scale these effects up to truly macroscopic numbers of photons (Watt-scale optical powers, with photon numbers of order  $10^{12}$ ). For definiteness, we consider a cavity formed by two highly-reflective and frequency-dependent end-mirrors arranged in a semi-confocal geometry (see Fig 2(e)). The higher the reflectivity of these mirrors, the lower the background losses. Inside is placed an etalon which is tilted to reflect light into the far-field, providing leakage. The resulting loss would be as if one of end mirrors had a transmittivity as depicted in Fig. 1(c). Inside the cavity is a nonlinear Kerr medium such as GaP or GaAs. For most of what we will consider, the single-photon nonlinearity provided in these macroscopic cases is extremely small ( $\beta$  of  $10^{-20}$  is typical, leading to characteristic frequency shifts of 1 part in  $10^6$  or  $10^7$  for intensities we consider). Nevertheless, significant noise reduction is still predicted.

To show this, we consider the evolution of the time-dependent probability of finding photons in some mode (e.g., a  $\text{TEM}_{00}$  mode) resulting from the loss coefficient  $\kappa(n)$  and loss derivative  $dL/dn$ , which are respectively shown in red and blue (Fig. 2(f)). For a coherent state with an initial mean number of photons below the approximate zero at  $n_0$  (about  $10^{13}$ , corresponding to

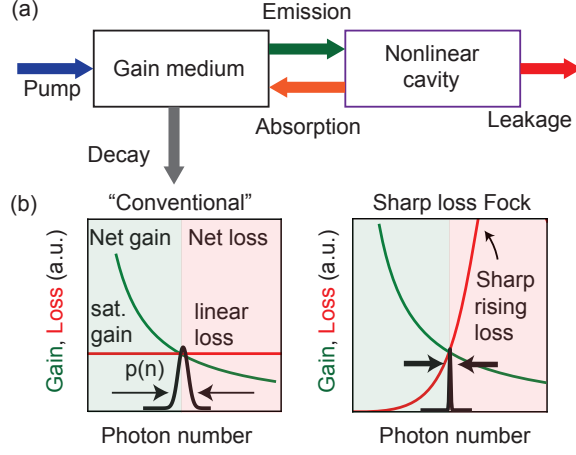


FIG. 3: **The Fock laser.** (a) Components of a general Fock laser, which consists of a pumped gain medium and a nonlinear cavity, interacting via absorption and emission of cavity photons by the gain medium. The cavity leakage is of the sharp form in Sec. I. (b, left) Saturable gain and linear loss (corresponding to a conventional laser) leads to Poissonian photon statistics well-above threshold. (b, right) On the other hand, saturable gain, combined with sharply rising loss, lead to condensation of the photon probability distribution, as in Fig. 1, except now in the steady-state.

an intracavity power of about 10 W), we see an increase in the noise (as expected from Eq. (2)) followed by convergence of the statistics to those of a coherent state. On the other hand, for an initial photon number above  $n_0$ , the variance transiently drops to a level about 90% below that of a coherent state, constituting macroscopic sub-Poissonian light. The background loss here is assumed to be  $10^4 \text{ s}^{-1}$ , requiring the end-mirrors to have reflectivities on the order of 99.999% (also therefore requiring high-finesse and actively stabilized cavities, similar to [36]). The main purpose of this result is to illustrate that the phenomena developed in this work do in fact extend to truly macroscopic regimes, and to show the types of requirements on such systems. Further reduction of the background loss by an order of magnitude leads to noise reduction of about 99%, while an order of magnitude larger background loss leads to noise reduction of 75%. It is worth pointing out that “even” 75% noise reduction of such a large state of light has not yet been realized, and represents an exciting goal for experimental realization [73].

### III. DIRECT PUMPING OF MACROSCOPIC SUB-POISSONIAN AND FOCK STATES OF LIGHT BY LASER ACTION

In all cases presented in the previous section, the low-noise state exists only transiently in the presence of finite background loss. Such states may already be of interest for some applications discussed earlier. However, it would be ideal to stabilize such states in time, leading to a large steady-state Fock or sub-Poissonian state of optical radiation. A natural idea to stabilize such states from the impact of loss is to introduce a gain medium which compensates for dissipation through stimulated emission. In this section, we introduce the concept of the “Fock laser,” which uses lasing action to stabilize a low-noise, or potentially Fock state.

The basic components of the Fock laser are shown in Fig. 3(a): it consists of a pumped gain medium with feedback from an optical resonator. Unlike conventional lasers in which the optical resonator has linear loss, the Fock laser makes use of a resonator with a sharply intensity dependent loss. This sharply increasing loss leads to a saturation mechanism for the laser that fundamentally differs from the saturation typically provided by gain saturation. To expand upon this, let us briefly review the celebrated quantum statistical theory of lasers developed by Scully and Lamb [37], which shows how the Poissonian (coherent-state) statistics arise from an interplay between gain saturation and linear loss. The Lamb-Scully theory concerns itself with systems for which the cavity decays more slowly than the inversion and polarization of the gain medium. The theory can thus be taken to always be valid for low-loss cavities, or media with fast  $T_1$  and  $T_2$  decays. In that case, it is possible to adiabatically eliminate the gain medium to derive the following equation of motion for the photon probabilities:

$$\begin{aligned} \dot{p}(n) = & G(n)p(n-1) - (G(n+1) + L(n))p(n) \\ & + L(n+1)p(n+1). \end{aligned} \quad (4)$$

Here  $G(n) = \frac{An}{1+n/n_s}$  is the stimulated emission rate by the gain medium into the lasing mode, with  $A$  the linear gain coefficient and  $n_s$  the saturation photon number (proportional to the saturation intensity). The linear gain coefficient is prescribed as  $A = S_0 R_{sp}$ , where  $S_0$  is the (unsaturated) population inversion and  $R_{sp} \sim c\sigma_{st}/V$  is the rate of spontaneous emission into the lasing mode (with  $\sigma_{st}$  the stimulated cross section of the gain medium and  $V$  the mode volume of the lasing mode). The steady-state of this equation is given by the cumulative product  $p(n) = \frac{1}{Z} \prod_{m=1}^n G(m)/L(m)$ , with  $Z$  a normalization constant ensuring  $\sum_n p(n) = 1$ . The mean number of photons  $\langle n \rangle$  is given

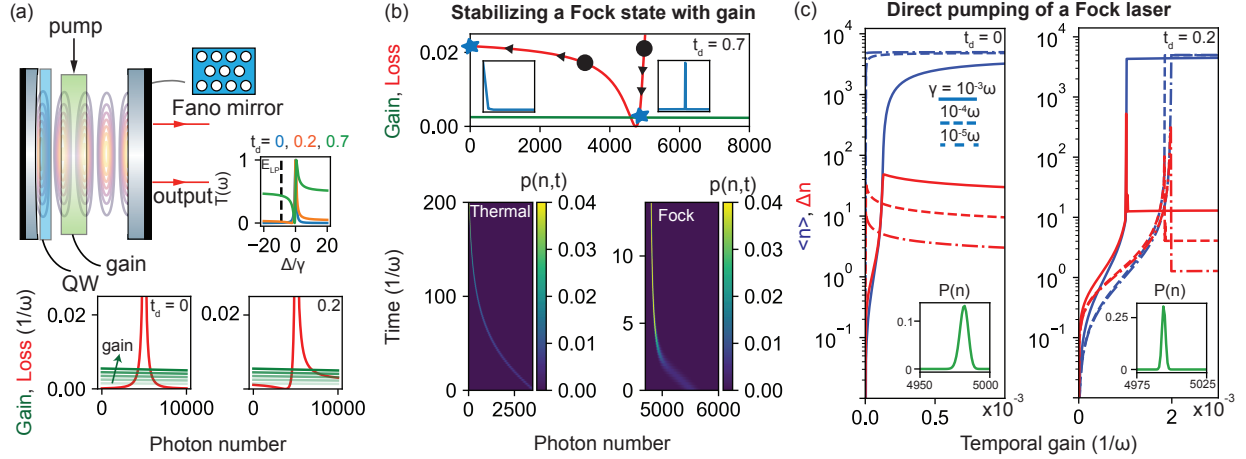


**FIG. 4: Fock lasing in systems with strong optical nonlinearities.** (a) The system of Fig. 2(a) is now converted into a “Fock laser” by inclusion of a gain medium. Different transmission profiles for the Fano mirror lead to different losses, and thus different emission-absorption diagrams. Note that  $t_d$  is the direct transmission coefficient that controls the Fano lineshape. (b) Evolution of an initial coherent state with different photon numbers (black circles) in the Fock laser. A state to the left of the approximate zero of the loss decays into a thermal state with a very low number of photons, while a state to the right of the zero decays into a steady-state with very low noise, approaching a high-number optical Fock state. (c) Photon number and fluctuations as a function of pump. “S-curves” similar to conventional lasers are observed in the photon number, except they saturate much more strongly, with the photon number hardly changing for increasing pump. Moreover, the photon number fluctuations, rather than increasing according to shot noise, decrease to nearly zero beyond threshold, indicating convergence to a near-Fock state. Different curves indicate different values of the mirror sharpness  $\gamma$ . Parameters regarding the excitonic nonlinearities and detunings are the same as in Fig. 2.

implicitly by the condition that the saturated gain equals the loss ( $G(\langle n \rangle) = L(\langle n \rangle)$ ), or graphically by the intersection of the gain and loss curves in an emission-absorption diagram (see Fig. 3(b)). We then find that the photon number uncertainty  $\Delta n$  is approximately given by (assuming  $\Delta n \gtrsim 1$ )

$$\Delta n = (1 - G(n+1)/L(n+1))^{-1/2}. \quad (5)$$

Eq. 5 states that the uncertainty in the photon number is dictated by how quickly the gain and/or loss vary around the equilibrium photon number (to see this, note that Eq. 5 may be written as  $\Delta n \approx (d(G/L)/dn)^{-1/2}$ ). For the case of saturable gain and linear loss, one immediately arrives

at  $(\Delta n) = \sqrt{n}$ , recovering Poissonian statistics (Fig. 3(b, left)). For a loss that varies rapidly, the noise will be brought down below the classical level (in a way that depends on  $dL/dn$ , as expected from the discussion of Eq. 2). For sufficiently sharp loss, the system will lase into a close approximation to a macroscopic Fock state (Fig. 3(b, right)), hence the nomenclature “Fock laser.”

We now show how the presence of a gain medium impacts the dynamics of the exciton-polariton system of Fig. 2(a). Suppose we incorporate into the cavity of Fig. 2(a) a gain medium (e.g., a pumped semiconductor gain medium), as shown in Fig. 4(a). Absorption and emission diagrams are shown for different transmission profiles for the Fano mirror: in each case, a sharp loss can be realized [38, 39]. Before considering “traditional lasing dynamics,” let us first consider how the dynamics presented in Fig. 2 – free decay of an initially coherent field – are changed when a gain medium is included (taken to be linear unsaturated gain with a gain quality factor of 1000). As before, initial states above  $n_0$  lead to close approximations to Fock states (here, the noise is 98% below the classical limit), while those below decay to low photon numbers (see Fig. 4(b)). In contrast to the case with no gain, the low-noise state which is created is a steady-state of the system. One point to note here is that the gain provided to the system is below threshold (see emission-absorption diagram in Fig. 4(b)). Specifically, if the system started with no excitations, the system would equilibrate to a thermal state with few photons (see inset of Fig. 4(b)). However, if the system is initialized with a number of photons above  $n_0$ , the gain balances the loss, because the loss is far lower near  $n_0$  than it is near  $n = 0$ . In principle, such a state could be realized by a protocol in which: (1) the cavity is pumped to support  $n > n_0$  excitations (2) the cavity pump is turned off while the pump of the gain medium is turned on before the field can decay.

The Fock laser may also be pumped directly from the vacuum state of the cavity provided that the gain exceeds the loss (at  $n = 0$ ), as it does in the emission/absorption diagrams shown in Fig. 4(a). In this case, as the pumping of the gain medium is increased, the system will hit a threshold at which the number of photons in the cavity mode rapidly increases, as one would expect for a generic laser. This is shown in Fig. 4(c), where we plot the intracavity photon number and the uncertainty as a function of the pump strength. While the behavior below and around threshold is similar to that of a “conventional” laser, the behavior beyond is quite different. In both panels of Fig. 4(c), one notices that beyond threshold, the photon number stays nearly constant as a function of increasing pump strength. For a conventional laser, one would expect the photon number to increase linearly with the pump. This difference is a result of the extreme saturation

(or alternatively, “negative feedback”) provided by the sharp loss: because the loss is so steep, increasing the gain (following the green arrow in Fig. 4(a)) negligibly changes the intersection point between gain and loss. The fluctuations are also markedly different from the conventional case, where they are expected to increase as  $\sqrt{n}$  as a function of increasing pump. Here instead, they *decrease* and then saturate at a very low value. For the most extreme case on the right panel of Fig. 4(c), the minimum uncertainty reached is 1. Thus the Fano factor is reduced by a factor of about 5,000, corresponding to a 5000-fold noise reduction below the shot-noise limit.

### A. Fock lasing in the macroscopic regime

Having shown in Sec. III that the sharp loss could lead to transient photon noise condensation even in macroscopic regimes, we now turn to the question of whether the Fock laser concept developed in the previous section could lead to similarly large noise condensation for macroscopic light in steady-state regimes. In particular, we show how existing gain media could be used with realistic cavity geometries to realize unprecedentedly large steady-state noise reductions. For concreteness, we consider a system of the type shown in Fig. 5, where we show a solid-state gain medium (here, Nd:YAG, which lases at 1064 nm) placed in the cavity of Fig. 2(e) which uses high-reflectivity end-mirrors (in a semi-confocal geometry) and an internal etalon as the out-coupler. Inside the 10 cm cavity is a Kerr nonlinear medium, (with  $n_2 = 1.2 \times 10^{-13} \text{ cm}^2/\text{W}$  [74]). Absorption-emission diagrams are shown in Fig. 5(b) for different pump strengths (for diode-based pumping at 808 nm, these correspond to pump intensities of 0.001, 0.05, and 0.2 kW/cm<sup>2</sup>, respectively).

Unlike the case of the laser medium considered in the previous section, Nd:YAG has an exceptionally slow inversion relaxation timescale (of 230  $\mu\text{s}$ ). As a result, it is not possible in all cases to adiabatically eliminate the population inversion from the quantum laser equations. In that case, we must follow the dynamics of the inversion and the cavity field simultaneously. While we cannot describe the cavity mode in terms of its reduced density matrix, we can still describe the dynamics of the system (and most importantly, its steady-state photon statistics) through a set of quantum operator Langevin equations for the photon number operator  $n$  and the population inversion operator  $S$  [40]. These operators evolve according to

$$\begin{aligned}\dot{n} &= (R_{\text{sp}}S - \kappa(n))n + F_n \\ \dot{S} &= \Lambda - (\gamma_{\parallel} + R_{\text{sp}}n)S + F_S,\end{aligned}\tag{6}$$

where  $\Lambda$  is the pumping rate of the gain medium and  $\gamma_{||}$  is the inversion relaxation rate (all other quantities were defined below Eq. 4). The equations take the form of the familiar rate equations for photon number and inversion, except for the presence of the quantum stochastic (Langevin) force terms  $F_n$  and  $F_S$ . These forces lead to fluctuations in the photon number and inversion from their mean values. The forces have zero mean, and correlation functions given by  $\langle F_i(t)F_j(t') \rangle = \langle 2D_{ij} \rangle \delta(t - t')$  with  $i, j = n, S$ . The diffusion coefficients,  $2D_{ij}$  are given by:

$$\begin{aligned} 2D_{nn} &= \langle (R_{sp}S + \kappa(n)) n \rangle \\ 2D_{nS} &= 2D_{Sn} = -\langle R_{sp}Sn \rangle \\ 2D_{SS} &= \Lambda + \langle (\gamma_{||} + R_{sp}n) S \rangle. \end{aligned} \quad (7)$$

To find the steady-state statistics of the field, we linearize Eq. 6 around the mean values, writing  $n = \langle n \rangle + \delta n$  and  $S = \langle S \rangle + \delta S$ . The fluctuations then satisfy the equation

$$\begin{pmatrix} \dot{\delta S} \\ \dot{\delta n} \end{pmatrix} = \begin{pmatrix} -(\gamma_{||} + R_{sp}\langle n \rangle) & -R_{sp}\langle S \rangle \\ R_{sp}\langle n \rangle & -\kappa'(\langle n \rangle)\langle n \rangle \end{pmatrix} \begin{pmatrix} \delta S \\ \delta n \end{pmatrix} + \begin{pmatrix} F_S \\ F_n \end{pmatrix}. \quad (8)$$

The main take-away from Eq. 8 is that the presence of a sharply increasing loss (which is the only “new” term in Eq. 6 compared to known treatments of fluctuations in lasers) *reduces* the fluctuations of  $\delta n$  (due to the sign of the term). Once again, we see the influence of the derivative of the loss ( $dL/dn$ ). To connect these equations to the quantum statistics, we note that the quantity  $S_a(\omega) = \frac{1}{\pi} \langle \delta n^\dagger(\omega) \delta n(\omega) \rangle$ , which is the intensity noise spectrum as measurable by a spectrum analyzer, is related to the photon-number uncertainty in the cavity by  $(\Delta n)^2 = \int_0^\infty d\omega S_a(\omega)$ .

Results are shown in Fig. 5(c). For low pumping intensities, where the gain intersects the loss curve where it is large but decreasing, the noise is hardly changed (in fact, it is slightly increased because  $\kappa'$  has the “wrong” sign). On the other hand, for larger pump intensities, the noise (at all frequencies) is significantly lowered. In the middle panel of Fig. 5(c), one sees that the noise can be reduced by nearly 80% below the classical shot noise limit (with even larger reductions of 30-fold, or about 15 dB for the low-frequency part of the noise spectrum). Interestingly, the noise reduction is not monotonic in pump strength, this is because eventually, the gain intersects the loss at a point which is effectively less sharp. Nevertheless, even in this simple example, large noise reductions arising from sharp loss are in principle achievable, in steady-state.



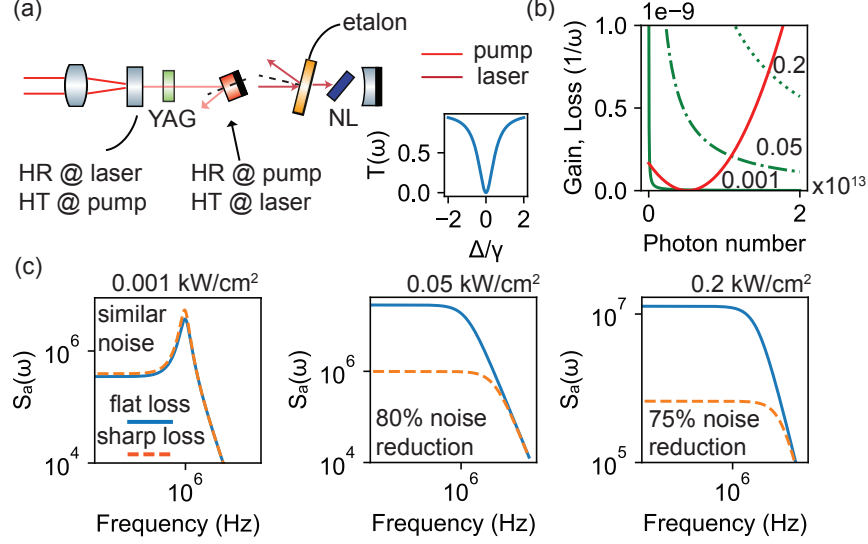


**FIG. 5: Fock lasers in the macroscopic regime and large suppression of photon noise in a common laser architecture.** (a) A macroscopic implementation of a Fock laser based on a diode-pumped solid-state laser with a sharply-varying transmissive element (e.g., an etalon) and a nonlinear crystal. (b) Absorption-emission diagrams for different pump intensities (0.001, 0.05, and 0.2 kW/cm<sup>2</sup>). (c) Cavity amplitude-noise spectra as a function of frequency for different pump intensities. For intermediate pump intensities, the overall noise reduction can be as high as 80% of the shot-noise limit with 10<sup>13</sup> photons. The frequency-dependent noise can be reduced by as much as 30-fold for low frequencies.

#### IV. DISCUSSION AND OUTLOOK

The discussion is divided into three main topics: relation to prior art, paths to experimental implementation, and potentially exciting research directions that stem from this work. We then provide a brief summary of the work.

*Relation to prior art.* Perhaps one of the most closely related concepts to the one presented here is that of “sub-Poissonian lasing” (theoretically and experimentally demonstrated in the 1980s, see Refs. [41–43] for examples and Ref. [44] for a comprehensive review). In sub-Poissonian lasing, one pumps a laser with a source that has very low pump fluctuations (such as an electrical current in a *pn*-junction in constant current operation). This low-noise pump is referred to as quiet pumping. The resulting output beam, in the far-field, can have noise below the shot-noise level in some range of frequencies. A number of differences emerge: besides the fact that nonlinearity is not employed, the maximum noise reduction that in principle possible is 50% in the cavity mode

(this is an upper bound, and was unlikely to have been reached). Meanwhile, the output beam, with lower noise, can only be claimed to be a sub-Poissonian state at specific noise frequencies (e.g., low frequencies characteristic of pump noise fluctuations), which is of course different from the fundamental Fock state of a single mode of light. Interestingly, in our results presented here, which consider conventional pumping (as opposed to quiet pumping): noise can still be quite suppressed at low frequencies, and the cavity noise reduction can be close to 100%, corresponding to orders-of-magnitude additional noise suppression, in some extreme cases producing something looking very much like a macroscopic Fock state of a cavity (the far-field beam remains a problem for further work).

Beyond this, there were several notable theoretical works considering the cavity statistics of lasers with embedded nonlinear absorbers [45–47] (e.g., saturable absorption, two-photon, and three-photon absorption). This is reasonable, as all of these effects lead to “negative feedback” which was long-known to lead to noise reduction (a recent proposal in superconducting qubits, which explains the idea, is presented in Ref. [48]). For low-order absorbers (second- and third-), the achievable noise reductions are modest ( $< 50\%$ ). High-order nonlinearities (larger than third) could in principle achieve further noise reductions [49, 50]. Perhaps mostly closely related to our work, Yariv and Vahala noted that frequency-dependent losses could lead to linewidth and amplitude noise suppression in the presence of amplitude-phase coupling (specific to semiconductor lasers [51, 52]). In all cases, these concepts would enrich the idea we present here: higher-order nonlinearities, as well as “quiet pumping”, would likely bring the achievable noise reduction very close to 100%, probably even in macroscopic cases. We would be remiss to not mention squeezing. The noise condensation effect shown here can be considered as an extreme-form of number squeezing (as opposed to the quadrature-squeezing of squeezed-vacuum achieved by  $\chi^{(2)}$  and  $\chi^{(3)}$  media). Number squeezing is also achievable through low-order nonlinearities by means of displacing a squeezed state. That said, a Fock state is fundamentally different from an amplitude-squeezed state [1]: a Fock state is not squeezed (it has large uncertainties in phase, and phase space volume  $(2n + 1)$ ). In a way, one of the important results of this work is that we have identified a nonlinearity that naturally produces Fock and other number-squeezed states of light (as well as suggested mechanisms to realize it).

*Paths to experimental realization.* Here, we briefly outline a few paths to experimental realization. There are of course many others. Regarding the strong-coupling realization: it is worth pointing out that the parameters we took to describe the gain and the nonlinearity in the exciton-

polariton case have all been achieved. The nonlinearities chosen are in fact even over an order-of-magnitude lower than reported in such systems [32, 34]. Larger nonlinearities, keeping all parameters the same, would reduce the size of the Fock state. The integration of a gain medium (such as an additional quantum well) and pump goes beyond what has presently been demonstrated but is in principle achievable.

Another important set of demonstrations includes the macroscopic cases shown in Fig. 2(e-h) and Fig. 5. We chose the example of Nd:YAG for concreteness, familiarity, and relative ease of theoretical description. We wholly expect that there are better lasing platforms to realize the physics proposed in this work. However, given the size of the design space, we have chosen a simple system somewhat arbitrarily for concreteness. For the gain medium, an obvious choice to consider is electrically pumped semiconductor gain media, which can provide rather high gain, need not be laser pumped, and can provide gain over a very broad frequency range, enabling compatibility with many different nonlinear materials. Another important advantage of semiconductor gain media is that they could be integrated into nanophotonic platforms which present high single-photon nonlinearities (at least 10 orders of magnitude higher than the bulk realizations presented, due to the correspondingly reduced mode volume [53]). Moreover, recent advances in nanophotonics enable the construction of very small, and very sharp transmissive elements (in particular, consider the recent developments in Fano resonances and bound states in the continuum in photonics, as well as earlier seminal work on high-Q photonic crystal defect cavities, as well as microsphere and microring cavities [54–57]). These small cavities could enable production of photon states with a small mean number but uncertainty well below 1 photon, looking more like a “true” Fock state. In terms of experimental realization, because the effects are optimized by having sharp loss, high nonlinearities, and regions of low loss: we expect that experimental observation of this effect will require mitigation of mechanical and thermal noise (via external-feedback stabilization techniques [58]), as well as noise arising from the pump (e.g., quiet pumping schemes, as applicable to semiconductors).

*Subsequent research directions.* Beyond the exciting experimental opportunities which could stem from this work, we should also list (in no particular order) a few areas of fundamental directions that would benefit from additional theoretical developments. One is the consideration of lasers with embedded nonlinearities formed by extreme nonlinearities, such as those arising from phenomena as strong coupling, as well as electromagnetically induced transparency (which leads to extremely high nonlinearities, even in bulk). The phenomena presented in this work could also

be extended to the microwave regime, where due to advances in circuit quantum electrodynamics, one can realize strong microwave nonlinearities using concepts of strong-, ultra-strong, and deep-strong quantum electrodynamical coupling [59–61]. One could also likely use such nonlinearities to engineer a *sharp gain* (rather than a sharp loss): a sharply decreasing gain should lead to similar effects of photon noise condensation as presented in this work. Another area to investigate is the properties of the far-field due to this nonlinearity, as well as the coherence properties of light produced in lasers with sharp nonlinear loss: could the linewidth be enhanced? Finally, due to the potentially macroscopic nature of the sub-Poissonian fields here, one may be able to use it to drive nonlinear optical processes (like harmonic generation, and perhaps one day, high-harmonic generation). There would in such case be a need for general theories of optical phenomena in systems strongly driven by non-Gaussian light.

*Summary.* To summarize, we have developed a quantum theory of photon noise in systems with sharply intensity-dependent optical losses (based on both reservoir theory, and Langevin theory). We have found an equation of motion which describes the evolution of the statistics in these cases, predicting the surprising result of nearly complete photon noise condensation, even in systems with macroscopic numbers of photons. We have presented systems that realize such models based on conservative Kerr nonlinearities and sharply frequency-dependent linear losses. We have considered several applications of this phenomenon: in one case, the transient generation of many-photon Fock states with thousands of photons, as well as macroscopic optical states (with multi-Watt optical powers) with noise far below the shot-noise limit. We showed that such states could even be maintained in the steady state by incorporating into the cavity a gain medium that stabilizes the low-noise state in an equilibrium between dissipation and stimulated emission, which we showed applied in both mesoscopic and macroscopic settings. Such a device constitutes a new type of laser (which we named the “Fock laser”) that employs a fundamentally different mechanism of saturation, leading to correspondingly different quantum statistics.

## V. METHODS

In this section, we give a broad overview of the theory of sharp intensity-dependent loss used to derive the results in this work. Complete derivations are provided in the Supplementary Information (SI).

### A. A physical system realizing the physics of Sec. II

Consider a system composed of an anharmonic oscillator (cavity mode), a single harmonic oscillator (constituting the resonance of one of the end mirrors; the other mirror is assumed to be perfectly reflecting), and a single reservoir comprised of a continuum of harmonic oscillators (reservoir). The anharmonic oscillator is coupled to the discrete oscillators, both of which are coupled to the reservoir. The system is described by the Hamiltonian

$$H/\hbar = H_a + \omega_d d^\dagger d + (\lambda a d^\dagger + \lambda^* a^\dagger d) + \sum_k \omega_k b_k^\dagger b_k + \sum_k \left( g_k a b_k^\dagger + g_k^* a^\dagger b_k \right) + \sum_k \left( v_k d b_k^\dagger + v_k^* d^\dagger b_k \right). \quad (9)$$

In this Hamiltonian,  $a, d, b_k$  are respectively the annihilation operators corresponding to the anharmonic oscillator, the mirror (of frequency  $\omega_d$ ) and the  $k$ th oscillator of the reservoir (of frequency  $\omega_k$ ). The quantities  $\lambda, g_k, v_k$  are respectively the cavity-to-mirror, cavity-to-reservoir, and mirror-to-reservoir couplings. The term  $H_a$  is the Hamiltonian of the anharmonic oscillator. In this manuscript, we will exclusively consider the case of an anharmonic oscillator with Kerr-type, or intensity-dependent, nonlinearities, in which the Hamiltonian may be written as  $H_{\text{anh}}/\hbar = \Omega(a^\dagger a) = \sum_{n=0}^{\infty} \Omega(n) |n\rangle \langle n|$ . The second equality indicates that the energy depends on the photon number  $n$  through the function  $\Omega(n)$ .

### B. Density-matrix description of an anharmonic oscillator with sharp losses

For the cases we consider, the coupling of  $a$  and  $d$  to the continuum are weak, and the oscillator-continuum couplings  $g_k$  and  $v_k$  can be taken as frequency independent ( $g_k \rightarrow g, v_k \rightarrow v$ ). In that case, the coupling of  $a$  and  $d$  to the common continuum is Markovian, and the density matrix of the system formed by  $a$  and  $d$ ,  $\rho_{ad}$  evolves according to

$$\dot{\rho}_{ad} = -i[H_{ad}/\hbar, \rho_{ad}] + (X^\dagger X \rho_{ad} + \rho_{ad} X^\dagger X - 2X \rho_{ad} X^\dagger). \quad (10)$$

Here, we have defined  $H_{ad} = H_{\text{anh}} + \omega_d d^\dagger d + \lambda a d^\dagger + \lambda^* a^\dagger d$  and  $X \equiv \sqrt{\kappa} a + \sqrt{\gamma} d$ , with  $\kappa$  the decay rate of the mode  $a$  and  $\gamma$  the decay rate of mode  $d$  [6].

To proceed, we will consider the case in which the resonance of the end-mirror  $d$  decays much faster than the cavity  $a$  (so  $\gamma \gg \kappa$ ). This describes a situation in which the end-mirror can respond instantaneously to changes in the state of  $a$ . Thus, if the photon number of  $a$  changes (and thus

its transition frequency  $\omega_{n,n-1}$ ), the end-mirror will respond to the instantaneous frequency of  $a$  (this is a type of adiabatic approximation). In this limit, the dynamics of the end-mirror can be adiabatically eliminated, and we can get a single equation for the reduced density matrix of  $a$ , denoted  $\rho$ . It is given by:

$$\begin{aligned}
\dot{\rho} = & -\kappa(a^\dagger a \rho + \rho a^\dagger a - 2a \rho a^\dagger) \\
& + \sum_{n=0}^{\infty} \frac{n G_+ G_-}{i(\omega_d - \omega_{n,n-1}) + \gamma} T_{n,n} \rho \\
& + \sum_{n=0}^{\infty} \frac{n (G_+ G_-)^*}{-i(\omega_d - \omega_{n,n-1}) + \gamma} \rho T_{n,n} \\
& + \sum_{m,n=0}^{\infty} \frac{\sqrt{m(n+1)} (G_+ G_-)^*}{-i(\omega_d - \omega_{n+1,n}) + \gamma} T_{m-1,m} \rho T_{n+1,n} \\
& + \sum_{m,n=0}^{\infty} \frac{\sqrt{m(n+1)} (G_+ G_-)}{i(\omega_d - \omega_{m,m-1}) + \gamma} T_{m-1,m} \rho T_{n+1,n},
\end{aligned} \tag{11}$$

where  $T_{i,j} = |i\rangle\langle j|$ ,  $G_- = i\lambda + \frac{1}{2}\sqrt{\kappa\gamma}$ , and  $G_+ = i\lambda^* + \frac{1}{2}\sqrt{\kappa\gamma}$ . This equation specifies not only the dynamics of the photon probabilities ( $p(n) = \rho_{n,n}$ ), which are relevant for Fock state generation, but also the dynamics of coherence between different states (off-diagonal components  $\rho_{n-k,n}$ ). This equation thus forms the basis for a theory of phase and amplitude coherence in nonlinear photonic systems with sharply frequency-dependent loss, and equations of motion for such coherences are shown in the SI. In the SI, we provide numerical support for this equation (for smaller systems of 100 photons, due to computational limitations). In the SI, we not only derive the full equation of motion for the reduced density matrix of  $a$ , but we also provide further validation of this model. This is carried out by numerically simulating the quantum dynamics of light governed by the Hamiltonian of Eq. (9) (for a single discrete oscillator). In particular, we directly simulate the time-evolution of the density matrix of the coupled oscillators assuming a Born-Markov description of the coupling of the two oscillators to a common bath (e.g., a radiation continuum). We then show that the evolution of the cavity oscillator state indeed follows the dynamics expected from the rate equation of Eq. (2), leading to phenomena of noise condensation presented in the text.

The equation of motion for the photon number probabilities can be found as

$$\begin{aligned}
\dot{\rho}_{n,n} = & -n \left( \kappa - 2\text{Re} \left[ \frac{G_+ G_-}{i(\omega_d - \omega_{n,n-1}) + \gamma/2} \right] \right) \rho_{n,n} + \\
& (n+1) \left( \kappa - 2\text{Re} \left[ \frac{G_+ G_-}{i(\omega_d - \omega_{n+1,n}) + \gamma/2} \right] \right) \rho_{n+1,n+1},
\end{aligned} \tag{12}$$

which is clearly of the form of Eq. (1) of the main text, with

$$L(n) = n \frac{vT(\omega_{n,n-1})}{2L_c}, \text{ where}$$

$$T(\omega) = \frac{|t_d|^2(\omega - \omega_d)^2 + |r_d|^2\gamma^2/4 + |r_d||t_d|\gamma(\omega - \omega_d)}{(\omega - \omega_d)^2 + \gamma^2/4}. \quad (13)$$

Here,  $v$  is the speed of light in the cavity, and  $L_c$  the cavity length. The transmission is identified as a Fano (asymmetric) transmission profile with the direct transmission and reflection coefficients identified in terms of the model parameters as  $t_d = \sqrt{\frac{2L\kappa}{c}}$  and  $r_d = \sqrt{\frac{8L}{\gamma c}}\lambda$ . This is done by comparing to results from the classical temporal-coupled mode theory of the Fano resonance (shown in SI). The content of this equation is expected to straightforwardly generalize to more complex multi-resonant end-mirrors: one simply uses the experimentally known transmission of the end-mirror, at the nonlinear frequency of the resonator.

As mentioned in the SI, Section S2, in a Kerr resonator, the excitation energy from a state with  $n - 1$  photons, to a state with  $n$  photons, is  $\omega_{n,n-1} = \omega(1 + 2\beta n)$ . The interaction constant,  $\beta$  is governed by the overlap integral between the (normalized) cavity mode  $\mathbf{u}(\mathbf{r})$  and the third-order nonlinear susceptibility  $\chi^{(3)}(\mathbf{r})$  (taken as a scalar here for simplicity). In particular  $\beta = \left(\frac{3\hbar\omega}{8\epsilon_0}\right) \int d^3r \chi^{(3)}(\mathbf{r})\mathbf{u}(\mathbf{r})^4$  (here we take real, standing-wave modes). Its characteristic magnitude, for a crystal which fills the cavity, is  $\frac{3\hbar\omega}{8\epsilon_0 V}\chi^{(3)}(\mathbf{r})$ , with  $V$  the mode volume.

To conclude this section, we comment on what happens in the opposite limit of the adiabatic elimination regime,  $\gamma \lesssim \kappa$ . In this case, excitations build up in the end-mirror, and so a given field strength in the coupled system corresponds to a smaller amplitude in the  $a$  cavity than expected, further reducing the nonlinear shift per photon. In this case, the nonlinearity could instead be integrated into the  $d$  cavity (consider a nonlinear photonic crystal mirror). This effectively interchanges the roles of  $a$  and  $d$ .

### C. Heisenberg-Langevin description of an anharmonic oscillator with sharp losses

This nonlinear dissipation can also be understood through the Heisenberg-Langevin framework, in which we may express the dynamics of the photon number operator in terms of a deterministic dissipative part and a quantum-fluctuating force associated with the reservoir. This force effectively enforces the fluctuation-dissipation theorem (alternatively, it may be thought of as preserving fundamental commutation relations between operators at all times). This Langevin description of the loss, for our purposes, is important for two reasons. For one, it enables us to

derive the quantum statistics of lasers based on this sharp loss, in cases where the usual density matrix theory cannot readily be applied (specifically, for lasers with slow inversion relaxation, such as solid-state, and sometimes semiconductor lasers). The other important point is that it effectively “completes” the quantum optical theory of sharp loss, in the sense that loss is typically described in quantum optics through two complementary frameworks: the density-matrix (master equation) approach and the Heisenberg-Langevin approach.

Derivations are given in the SI: here, we state the main steps and final result. The equation (1) (or equivalently (12)) can be taken to correspond to a Heisenberg-Langevin equation of the form:

$$\dot{T}_{n,n} = -L_n T_{n,n} + L_{n+1} T_{n+1,n+1} + F_{n,n}, \quad (14)$$

where  $F_{n,n}$  are operator valued forces associated with the effect of the reservoir (with operators  $b_k$  and  $d$ ) defined in Eq. (3). The force is assumed to have zero mean but finite second-order correlations that are delta-correlated (schematically  $\langle F(t)F(t') \rangle = 2D\delta(t-t')$  for some operator-valued “diffusion coefficient”  $D$ ).

The correlation functions between different forces (e.g.,  $F_\mu, F_\nu$ ), corresponding to the equations of motion for operators  $A_\mu, A_\nu$  – provided they have zero mean and are delta-correlated in time (memory-less) – satisfy the so-called Einstein-relation for the diffusion coefficient  $D_{\mu\nu}$  (defined so that  $\langle F_\mu(t)F_\nu(t') \rangle \equiv 2\langle D_{\mu\nu} \rangle \delta(t-t')$ ):

$$2\langle D_{\mu\nu} \rangle = \frac{d}{dt} \langle A_\mu A_\nu \rangle - \langle A_\mu D_\nu \rangle - \langle D_\mu A_\nu \rangle, \quad (15)$$

The drift term,  $D_\mu$  is defined such that  $\dot{A}_\mu = D_\mu + F_\mu$ . After some algebra, the diffusion coefficient is found to be

$$2\langle D_{n,n} \rangle = \langle L(n) \rangle = \langle n\kappa(n) \rangle, \quad (16)$$

where  $L(n) = n\kappa(n)$  is understood to be a function of the  $n$ -operator. Equations (14) and (16) may then be used to derive an equation of motion for the photon number operator  $n = \sum_{n=0}^{\infty} nT_{n,n}$ . The final result, derived in the SI, is shown to be

$$\dot{n} = -\kappa(n)n + F_n. \quad (17)$$

The photon number force  $F_n$  satisfies

$$\begin{aligned} \langle F_n(t) \rangle &= 0 \\ \langle F_n(t)F_n(t') \rangle &= \langle L(n) \rangle \delta(t-t'), \end{aligned} \quad (18)$$

where  $L(n)$  is for example given by Eq. (3) of the main text generally (and Eq. (13) for the specific model from Methods Sec. A).



## Appendix A: Introduction to Supplementary Materials

In this Supplement, we provide a rigorous quantum optical derivation and extend all results used in the main text. In Section B, we will derive the Hamiltonian of the laser model that we consider: gain based on effectively two-level gain media, coupled to a nonlinear cavity with one perfectly reflecting mirror, and one mirror with a Fano transmission profile. In Section C, we develop the general theory of loss in an anharmonic oscillator coupled to frequency-dependent loss, showing how a non-perturbative nonlinear loss emerges. This is done based on a density-matrix theory of damping. We then derive a corresponding Langevin theory of loss in such systems, which we use when deriving the quantum statistics of lasers with sharp-loss integrated within. This formalism leads to the rate equations used to calculate the photon statistics of the laser cavity field in Section III. In Section D, we lay out the basic equations governing the quantum statistical properties of lasers with sharp intensity-dependent losses, considering both regimes in which the population inversion decays quickly and slowly compared to the cavity lifetime. This enables us to consider the dynamics of most gain media used in conventional lasers: gases, molecular dyes, solid-state gain media, and semiconductors with Bloch electrons.

In this Supplement, with regard to “standard results”, we will typically cite them, rather than give a self-contained derivation of them. Thus, this Supplement will primarily focus on presenting “main equations” (as opposed to in-line equations) that are either new, or are intermediate steps towards deriving new results (those related to anharmonic oscillators with sharply dependent loss and their applications to lasers).

## Appendix B: Quantum theory of a nonlinear resonator with frequency-dependent loss

The starting point in our analysis of loss in a nonlinear resonator with frequency-dependent loss is the specification of the Hamiltonian, which describes the nonlinear cavity, the frequency-dependent end-mirror, and all reservoirs responsible for dissipation of the photon. Let us describe each term in the total Hamiltonian in steps.

*Nonlinear cavity.* Let us start by describing the cavity. We will assume in all cases that we are under conditions of single-mode lasing, and can thus consider the electromagnetic field of the cavity as described by a single high- $Q$  resonant mode. In the absence of photon nonlinearity, the Hamiltonian of the cavity would be simply  $\hbar\omega a^\dagger a$ , with  $\hbar$  the reduced Planck constant,  $\omega$  the

frequency of the resonant mode, and  $a$  ( $a^\dagger$ ) the annihilation (creation) operator of the cavity mode. Let us consider now what happens when a nonlinear element is introduced into the cavity.

Consider for example the case of a nonlinear crystal embedded in the cavity, leading to Kerr nonlinear shifts of the cavity frequency. The resulting cavity Hamiltonian can be written in the form  $H_{\text{Kerr}} = \hbar\omega a^\dagger a + \frac{1}{6}\beta\hbar\omega : (a - a^\dagger)^4 :$  [Drummond and Walls], where  $\beta$  is a nonlinear coupling constant, and  $::$  denotes normal ordering. In the rotating-wave approximation (i.e., ignoring terms with unbalanced numbers of creation and annihilation operators), the Kerr nonlinearity takes the more commonly stated form  $H_{\text{Kerr}} = \hbar\omega ((1 + \beta)a^\dagger a + \beta(a^\dagger a)^2)$  [27, 28]. The cavity eigenstates are Fock states of  $n$  photons with energy  $E_n \equiv \hbar\omega_n = \hbar\omega [(1 + \beta)n + \beta n^2]$ . With the spectrum established, the Hamiltonian, in the number basis, may alternatively be written as

$$H_{\text{Kerr}} = \sum_{n=0}^{\infty} E_n T_{n,n}, \quad (\text{B1})$$

with  $T$  a projection operator (projector), which is generally defined as:  $T_{i,j} \equiv |i\rangle\langle j|$ . We have re-written the Hamiltonian in terms of projectors, as they will play an essential role in our theory of nonlinear lasers. Before moving on to the theory of nonlinear lasers, we point out that in this Kerr resonator, the excitation energy from a state with  $n - 1$  photons, to a state with  $n$  photons, is  $\omega_{n,n-1} = \omega(1 + 2\beta n)$ . This is equivalent to the statement in classical nonlinear optics that the frequency of a nonlinear cavity shifts by an amount proportional to the intensity [30]. The interaction constant,  $\beta$  is governed by the overlap integral between the (normalized) cavity mode  $\mathbf{u}(\mathbf{r})$  and the third-order nonlinear susceptibility  $\chi^{(3)}(\mathbf{r})$  (taken as a scalar here for simplicity). In particular  $\beta = \left(\frac{3\hbar\omega}{8\epsilon_0}\right) \int d^3r \chi^{(3)}(\mathbf{r}) \mathbf{u}(\mathbf{r})^4$  (here we take real, standing-wave modes). Its characteristic magnitude, for a crystal which fills the cavity, is  $\frac{3\hbar\omega}{8\epsilon_0 V} \chi^{(3)}(\mathbf{r})$ , with  $V$  the mode volume. Before moving on to discuss the other terms in the Hamiltonian, we note that a general *intensity-sensitive* nonlinear cavity will have a Hamiltonian of the form of Eq. (1) with the appropriate photon-number-dependent energies, and so our treatment applies more generally than to the case of Kerr nonlinearities.

*Cavity losses.* Now we move to a discussion of the terms in the Hamiltonian responsible for the losses of the cavity. For the photon, the reservoirs depend on the exact configuration. In the simplest case we consider, the photon is coupled to a single reservoir of far-field modes which convert the cavity photon into the emitted beam. In the more complex case of the Fano laser that we discuss in Section D, we must introduce the internal resonant mode of the Fano mirror, its coupling to the laser cavity mode, and couplings of the far-field to both the Fano mirror *and* the

laser cavity. This approach was recently used to describe the quantum optics of Fano mirrors in [62]. The latter coupling represents “direct” coupling of the cavity to the far-field, and can lead to interference effects and a Fano lineshape for the transmission, as is well-known in classical optics. In what follows, we consider the more general case of the Fano mirror, and discuss the limiting case of a conventional (Fabry-Perot) mirror. Let us consider a situation in which our laser cavity mode (described by  $a$ ) is coupled to a second mode (e.g., a Fabry-Perot type mode, or a photonic crystal resonance), of frequency  $\omega_d$ , described by annihilation (creation) operators  $d$  ( $d^\dagger$ ). Its corresponding Hamiltonian is  $H_d = \hbar\omega_d d^\dagger d$ . The two modes are coupled by a term  $\hbar(\lambda a d^\dagger + \lambda^* a^\dagger d)$ . These modes however are also coupled to the continuum of far-field modes  $b_k$  outside of the cavity, where  $k$  enumerates over the continuum of outside modes. For simplicity, we will consider a one-sided cavity, with one wall perfectly reflecting, and one partially reflecting (see Fig. S1). Both the  $a$  and  $d$  modes can couple to the far-field modes, thus leaking out. Referring to the coupling constants of  $a$  and  $d$  to  $b_k$  as  $g_k$  and  $v_k$  respectively, we add the following reservoir Hamiltonian:  $H_{\text{res}} = \sum_k \hbar g_k (a b_k^\dagger + a^\dagger b_k) + \sum_k \hbar v_k (d b_k^\dagger + d^\dagger b_k)$ . Thus, the terms introduced by the internal mode, its coupling to the laser cavity, and far-field leakage, add to

$$H/\hbar = H_a + \omega_d d^\dagger d + (\lambda a d^\dagger + \lambda^* a^\dagger d) + \sum_k \omega_k b_k^\dagger b_k + \sum_k (g_k a b_k^\dagger + g_k^* a^\dagger b_k) + \sum_k (v_k d b_k^\dagger + v_k^* d^\dagger b_k), \quad (\text{B2})$$

where  $H_a$  is the Hamiltonian of the nonlinear cavity mode. The simpler case of a Fabry-Perot mirror (with a symmetric transmission spectrum) is obtained in the limit where the “direct” coupling of the cavity mode to the far-field can be neglected:  $g_k = 0$ , so that the cavity must couple through the mirror if it is to escape into the far-field. The other important standard case is that in which the partially reflecting mirror has a frequency independent reflectivity, which corresponds to the case in which the  $d$  cavity has a very fast decay. In this case, the  $d$  mode is ill-defined, and acts as if it is not a degree of freedom in the problem, leaving us only with the term  $\sum_k \hbar g_k (a b_k^\dagger + a^\dagger b_k)$ , which is typically used to describe dissipation in conventional lasers.

We note that in practice, while the parameters  $\lambda, g_k, v_k$  could be calculated, it is typically impractical to do so, and they may be found by comparing the transmission of the cavity to what is expected from a classical treatment of the cavity transmission (from temporal coupled mode theory).

## 1. Density matrix description of a nonlinear resonator with loss

In this section, we derive a master equation to describe the damping of a nonlinear resonator ( $a$ ) due to radiative leakage from a frequency-dependent mirror. The overall Hamiltonian of the system+reservoir (resonator + end-mirror + reservoir) is given by Eq. (2). To simplify notation, we will define

$$H_{ad} \equiv H_a + \omega_d d^\dagger d + (\lambda a d^\dagger + \lambda^* a^\dagger d). \quad (\text{B3})$$

Let us now derive an equation of motion for the reduced density matrix of  $a$  and  $d$  (e.g., tracing out the reservoir). Let us define the interaction picture:  $\rho_I = e^{iH_0 t} \rho e^{-iH_0 t}$  and  $V_I = e^{iH_0 t} V e^{-iH_0 t}$ , with  $H_0 = H_{ad} + \sum_k \omega_k b_k^\dagger b_k$  and  $V = \sum_k (g_k a b_k^\dagger + g_k^* a^\dagger b_k) + \sum_k (v_k d b_k^\dagger + v_k^* d^\dagger b_k)$ . Then, the equation of motion for the density matrix becomes  $\dot{\rho}_I = -i[V_I, \rho_I]$ , admitting the iterative solution:

$$\dot{\rho}_I = -i[V_I(t), \rho(0)] - \int_0^t dt' [V_I(t), [V_I(t'), \rho_I(t')]], \quad (\text{B4})$$

with  $\rho(0) = \rho_I(0)$  being the initial state of the system and reservoir. As we will primarily be interested in the application of this framework at optical frequencies, we will consider the reservoir to be in its vacuum state. The dynamics of the resonator and end-mirror are obtained by taking the partial trace with respect to the bath ( $\dot{\rho}_{ad} \equiv \text{tr}_b \rho$ ), such that

$$\dot{\rho}_{ad,I} = -i \text{tr}_b ([V_I(t), \rho(0)]) - \int_0^t dt' \text{tr}_b ([V_I(t), [V_I(t'), \rho_I(t')]]), \quad (\text{B5})$$

Upon taking the trace with respect to the bath, the term which is linear in  $V_I$  will vanish, and the equation of motion becomes

$$\dot{\rho}_{ad,I} = - \int_0^t dt' \text{tr}_b (V_I(t) V_I(t') \rho_I(t') + \rho_I(t') V_I(t') V_I(t) - V_I(t) \rho_I(t') V_I(t') - V_I(t') \rho_I(t') V_I(t)). \quad (\text{B6})$$

To proceed, we need further approximations. As the coupling of system and reservoir is weak, and the continuum of radiation modes loses memory over a very short timescale (due to its infinite bandwidth), we may make the standard Markov approximation. Namely, that  $\rho$  factorizes as  $\rho_I(t') = \rho_{ad,I}(t') \rho_b(0)$ , with  $\rho_b$  the density matrix of the multimode vacuum reservoir. Moreover, due to the weak coupling of  $a$  and  $d$  to the reservoir, the system-reservoir couplings can be approximated as frequency-independent (such that  $g_k \approx g$  and  $v_k \approx v$ ).

To simplify the evaluation of the terms in the previous equation, it will be convenient to define  $X = ga + vd$ . It follows that the first term, under these approximations, evaluates to  $X_I(t)X_I^\dagger(t')\rho_{ad}(t')\sum_k e^{i\omega_k(t-t')} = X_I(t)X_I^\dagger(t')\rho_{ad}(t')(2\pi\rho_0\delta(t-t'))$ , with  $\rho_0$  the density of states of the far-field continuum (which under these approximations is frequency-independent). Performing the time-integration yields  $X_I(t)X_I^\dagger(t)\rho_{ad}(t)$ . The other terms evaluate in a similar fashion, yielding

$$\dot{\rho}_{ad,I} = -2\pi\rho_0 \left( X_I^\dagger(t)X_I(t)\rho_{ad,I}(t) + \rho_{ad,I}(t)X_I^\dagger(t)X_I(t) - 2X_I(t)\rho_{ad,I}(t)X_I^\dagger(t) \right). \quad (\text{B7})$$

Going back into the Schrodinger picture, one has the equation of motion for the system (resonator + end-mirror)

$$\dot{\rho} = -i[H_{ad}, \rho] - 2\pi\rho_0 \left( X_I^\dagger X_I \rho + \rho X_I^\dagger X_I - 2X_I \rho X_I^\dagger \right), \quad (\text{B8})$$

where we have taken  $\rho_{ad} \rightarrow \rho$  for simplicity of notation (the bath will no longer enter the equations).

We are mainly interested in the limit in which the end-mirror responds instantaneously to changes in the frequency of the cavity mode. In other words, in the limit of  $\gamma \equiv 2\pi\rho_0 v^2$  being the fastest timescale of the problem (so for example,  $\gamma \gg \kappa \equiv 2\pi\rho_0 g^2$ ). Under this condition, we may adiabatically eliminate  $d$  from the master equation of Eq. (8), getting an equation of motion for  $a$  alone. The adiabatic elimination proceeds along similar lines to the derivation of Eq. (8): we must look at the evolution of the cavity density matrix to second-order in the cavity-mirror coupling. Thus, we want an equation similar to Eq. (5). A major difference in execution arises from the fact that the free dynamics of the end-mirror include damping (which is “fast”), and so the interaction-picture transformation must include the effect of damping. While interaction picture transformations of Liouvillians with Lindblad terms are a “basic” part of density-matrix theory, it is relatively uncommon in the literature ([63] provides a good account). Thus, we provide more of the intermediate manipulations than in other sections of the SI.

The equation of motion for the density matrix (in the Schrodinger picture) may be written as

$$\dot{\rho} = (\mathcal{L}_0 + \mathcal{L}_1)\rho, \quad (\text{B9})$$

where

$$\mathcal{L}_0 \equiv -i[H_a + \omega_d d^\dagger d, \cdot] - \gamma(d^\dagger d \cdot + \cdot d^\dagger d - 2d^\dagger \cdot d), \quad (\text{B10})$$

and

$$\begin{aligned}\mathcal{L}_1 \equiv & -i[\lambda ad^\dagger + \lambda^* a^\dagger d, \cdot] - \kappa(a^\dagger a \cdot + \cdot a^\dagger a - 2a^\dagger \cdot a) \\ & - \sqrt{\kappa\gamma}((ad^\dagger + a^\dagger d) \cdot + \cdot (ad^\dagger + a^\dagger d) - 2(a \cdot d^\dagger + d \cdot a^\dagger)).\end{aligned}\quad (\text{B11})$$

Here, we have introduced the  $\cdot$  notation, which indicates how the Liouvillian acts on an operator. For example, for arbitrary operators  $X, \rho$ , we have:  $(X \cdot) \rho \equiv X \rho$  and  $(\cdot X) \rho = \rho X$ . Terms of the form  $(X \cdot Y) \rho$ , for arbitrary  $X, Y$  should be understood as  $(X \cdot)(\cdot Y) \rho = X \rho Y$ . The terms Eq. (11) may also be regrouped to read as:

$$\begin{aligned}\mathcal{L}_1 = & -\kappa(a^\dagger a \cdot + \cdot a^\dagger a - 2a^\dagger \cdot a) \\ & - (G_-(ad^\dagger \cdot) + G_-^*(\cdot a^\dagger d)) - (G_+(a^\dagger d) + G_+(\cdot ad^\dagger)) + 2\sqrt{\kappa\gamma}(a \cdot d^\dagger + d \cdot a^\dagger),\end{aligned}\quad (\text{B12})$$

with  $G_- \equiv i\lambda + \sqrt{\kappa\gamma}$  and  $G_+ \equiv i\lambda^* + \sqrt{\kappa\gamma}$ . This expression proves more convenient for the manipulations that follow.

We now define the interaction picture density matrix  $\rho_I$  as

$$\rho = e^{\mathcal{L}_0 t} \rho_I, \quad (\text{B13})$$

so that

$$\dot{\rho}_I = e^{-\mathcal{L}_0 t} \mathcal{L}_1 e^{\mathcal{L}_0 t} \rho_I \equiv \mathcal{L}_I(t) \rho_I. \quad (\text{B14})$$

This equation admits an iterative solution of the form

$$\dot{\rho}_{a,I} = \text{tr}_d[\mathcal{L}_I(t) \rho_I(0)] + \int_0^t dt' \text{tr}_d[\mathcal{L}_I(t) \mathcal{L}_I(t') \rho_I(t')]. \quad (\text{B15})$$

This equation is considerably simplified in the limit where  $\gamma$  is large: in this case, the end-mirror acts as a broad continuum for the  $a$  mode (in other words, as a reservoir). Moreover, the end-mirror cannot sustain any build-up of excitations, as they damp immediately (on any timescale related to  $a$ ). It follows that from the perspective of the cavity mode, the end-mirror acts as a vacuum reservoir  $|0\rangle\langle 0|$ , and that the state of the cavity and mirror may be written in factorizable form:  $\rho_I(t) \approx \rho_{a,I}(t) |0\rangle\langle 0|$ . This allows us to write Eq. (15) in the Born-Markov approximation as

$$\dot{\rho}_{a,I} = \text{tr}_d[\mathcal{L}_I(t) \rho_a(t) |0\rangle\langle 0|] + \int_0^t dt' \text{tr}_d[\mathcal{L}_I(t) \mathcal{L}_I(t') \rho_a(t') |0\rangle\langle 0|]. \quad (\text{B16})$$

Here, we have also made an adiabatic approximation, replacing  $\rho_a(t')$  with  $\rho_a(t)$ , since significant contributions to the integrand only arise when  $t'$  is within  $\gamma^{-1}$  of  $t$ . Over this range of times, the

mirror density matrix does not vary. To proceed, we must now evaluate the interaction picture Liouvillian operators to second-order, and then evaluate the integrals that arise. The following interaction-picture transformations for  $d$  are used heavily in what follows [see Carmichael]:

$$\begin{aligned}
(d\cdot)_I(t) &= e^{-i\omega_d t - \gamma t}(d\cdot) \\
(\cdot d^\dagger)_I(t) &= [(\cdot d)_I(t)]^\dagger = e^{i\omega_d t - \gamma t}(\cdot d^\dagger) \\
(d^\dagger\cdot)_I(t) &= e^{i\omega_d t} (e^{\gamma t}(d^\dagger\cdot) + (e^{-\gamma t} - e^{\gamma t})(\cdot d^\dagger)) \\
(\cdot d)_I(t) &= [(d^\dagger\cdot)_I(t)]^\dagger = e^{-i\omega_d t} (e^{\gamma t}(\cdot d) + (e^{-\gamma t} - e^{\gamma t})(d\cdot)).
\end{aligned} \tag{B17}$$

Similarly, the interaction picture transformations for  $a$  are given as

$$\begin{aligned}
(a\cdot)_I(t) &= [(\cdot a^\dagger)_I(t)]^\dagger = \sum_{n=0}^{\infty} \sqrt{n} e^{-i\omega_{n,n-1}t} (T_{n-1,n}\cdot) \\
(a^\dagger\cdot)_I(t) &= [(\cdot a)_I(t)]^\dagger = \sum_{n=0}^{\infty} \sqrt{n+1} e^{i\omega_{n+1,n}t} (T_{n+1,n}\cdot),
\end{aligned} \tag{B18}$$

where we have defined the projector  $T_{ij} = |i\rangle\langle j|$ . Note that due to the polychromatic nature of  $a$  (being anharmonic), this is the most convenient way to express the interaction picture operator. With these identities established, we now evaluate the first- and second-order terms of Eq. (14).

As the end-mirror is in the vacuum state, no terms in  $\mathcal{L}_1$  involving  $d$  or  $d^\dagger$  contribute to the first-order term. Therefore, the first order term is simply  $-\kappa(a_I^\dagger a_I \cdot + \cdot a_I^\dagger a_I - 2a_I^\dagger \cdot a_I)$ , and in the Schrodinger picture, simply gives the expected term  $-\kappa(a^\dagger a \cdot + \cdot a^\dagger a - 2a^\dagger \cdot a)$ . Now we evaluate the second-order term.

To proceed, we note that since  $\gamma \gg \kappa$ , we may neglect contributions of order greater than  $\kappa$ . Hence, we may completely ignore the first line of Eq. (12) for the purposes of evaluating the second-order term. After algebra, one finds that the second order integrand is given (under the assumption that  $d$  is in the vacuum state) by:

$$\begin{aligned}
&-|G_-|^2 \text{tr}_d \left[ a_I(t) d_I^\dagger(t) \rho_a(t) |0\rangle\langle 0| a_I^\dagger(t') d_I(t') \right] - G_+ G_- \text{tr}_d \left[ a_I^\dagger(t) d_I(t) a_I(t') d_I^\dagger(t') \rho_a(t) |0\rangle\langle 0| \right] \\
&-|G_-|^2 \text{tr}_d \left[ a_I(t') d_I^\dagger(t') \rho_a(t) |0\rangle\langle 0| a_I^\dagger(t) d_I(t) \right] - (G_+ G_-)^* \text{tr}_d \left[ \rho_a(t) |0\rangle\langle 0| a_I^\dagger(t') d_I(t') a_I(t) d_I^\dagger(t) \right] \\
&+ 2\sqrt{\kappa\gamma} \text{tr}_d \left[ a_I(t) \rho_a(t) |0\rangle\langle 0| a_I^\dagger(t') d_I(t') d_I^\dagger(t) \right] + 2\sqrt{\kappa\gamma} \text{tr}_d \left[ d_I(t) a_I(t') d_I^\dagger(t') \rho_a(t) |0\rangle\langle 0| a_I^\dagger(t) \right].
\end{aligned} \tag{B19}$$

Plugging in the interaction picture operators of Eqs. (17) and (18), and evaluating the  $t'$ -integral,

one arrives at the following final result (in the Schrodinger picture):

$$\begin{aligned}
\dot{\rho} = & -\kappa(a^\dagger a \rho + \rho a^\dagger a - 2a \rho a^\dagger) \\
& + \sum_{n=0}^{\infty} \frac{n G_+ G_-}{i(\omega_d - \omega_{n,n-1}) + \gamma} T_{n,n} \rho + \sum_{n=0}^{\infty} \frac{n (G_+ G_-)^*}{-i(\omega_d - \omega_{n,n-1}) + \gamma} \rho T_{n,n} \\
& + \sum_{m,n=0}^{\infty} \frac{\sqrt{m(n+1)} (G_+ G_-)^*}{-i(\omega_d - \omega_{n+1,n}) + \gamma} T_{m-1,m} \rho T_{n+1,n} + \sum_{m,n=0}^{\infty} \frac{\sqrt{m(n+1)} (G_+ G_-)}{i(\omega_d - \omega_{m,m-1}) + \gamma} T_{m-1,m} \rho T_{n+1,n}.
\end{aligned} \tag{B20}$$

Here, we have taken  $\rho_a \rightarrow \rho$ , as no further reference will be made to the density operator of the end-mirror. Eq. (20) could be considered the main theoretical result of this work: it prescribes the dissipation dynamics of an anharmonic oscillator subject to dispersive loss. The equation governs the evolution of the entire density matrix of the anharmonic oscillator: not only the evolution of the populations (which are important for Fock state generation), but also the quantum coherences between different photonic states, which are important for monitoring the build-up and decay of phase and intensity correlations.

To connect to the results of the main text, let us now find an equation of motion for the populations  $\dot{\rho}_{n,n}$ . Taking the  $n, n$  matrix element of Eq. (20), one immediately finds

$$\begin{aligned}
\dot{\rho}_{n,n} = & -n \left( 2\kappa - \frac{G_+ G_-}{i(\omega_d - \omega_{n,n-1}) + \gamma} - \frac{(G_+ G_-)^*}{-i(\omega_d - \omega_{n,n-1}) + \gamma} \right) \rho_{n,n} \\
& + (n+1) \left( 2\kappa - \frac{G_+ G_-}{i(\omega_d - \omega_{n+1,n}) + \gamma} - \frac{(G_+ G_-)^*}{-i(\omega_d - \omega_{n+1,n}) + \gamma} \right) \rho_{n+1,n+1},
\end{aligned} \tag{B21}$$

which is clearly of the form

$$\dot{\rho}_{n,n} = -L_n \rho_{n,n} + L_{n+1} \rho_{n+1,n+1}, \tag{B22}$$

establishing the validity of Eq. (1) of the main text (noting that  $p(n) \equiv \rho_{n,n}$ ). To proceed, we will make the changes of definition  $\kappa \rightarrow \kappa/2$  and  $\gamma \rightarrow \gamma/2$  (in other words, we are changing  $\kappa, \gamma$  from the amplitude decay rate to the energy decay rate).

#### a. Physical interpretation of the loss terms

Now we establish the relationship to Eq. (4) of the main text. To do this, we note that the loss can be manipulated into the form:

$$L_n = n \left( \frac{\kappa \delta_n^2 + \gamma |\lambda|^2 + 2\sqrt{\kappa\gamma} \delta_n |\lambda| \cos \phi}{\delta_n^2 + \gamma^2/4} \right), \tag{B23}$$



with  $\delta_n \equiv \omega_{n,n-1} - \omega_d$ , and  $\lambda \equiv |\lambda|e^{i\phi}$ . To get a physical feeling for this expression, let us consider a related problem: the transmission and reflection of classical light scattering from a Fano mirror (a system with a Fano resonance). This problem has been studied by many authors, and is commonly considered in the field of nanophotonics. Consider a wave incident on a Fano mirror surrounded by air (e.g., a photonic crystal mirror). The wave has frequency  $\omega$ , the Fano mirror has frequency  $\omega_0$ , and radiative losses governed by the amplitude decay time  $2/\gamma$  with  $\gamma$  the energy decay rate. It can be shown [38, 39] that the energy transmission coefficient is then given by

$$T = \frac{|t_d|^2 \delta^2 + |r_d|^2 \gamma^2 / 4 \pm |r_d t_d| \gamma \delta}{\delta^2 + \gamma^2 / 4}, \quad (\text{B24})$$

with  $\delta = \omega - \omega_0$  and  $r_d, t_d$  representing reflection and transmission coefficients associated with the *direct* reflection and transmission of the incident light (i.e., without coupling into the internal mode of the mirror). These direct channels interfere with the indirect channel. Here, the  $\pm$  denotes the case of an even/odd mode. Comparing this with Eq. (23), we see that the losses are quite similar in form. In fact, we see that by taking Eq. (24) and applying:  $\omega \rightarrow \omega_{n,n-1}, \gamma \rightarrow \gamma, |t_d| \rightarrow \sqrt{\frac{2L\kappa}{c}}, |r_d| \rightarrow \sqrt{\frac{8L}{c\gamma}}|\lambda|$ , with  $L$  the length of the cavity supporting mode  $a$ , we have:

$$T_n \equiv T(\omega_{n,n-1}) = \frac{2L}{c} \frac{\kappa \delta_n^2 + \gamma |\lambda|^2 \pm 2\sqrt{\kappa\gamma} \delta_n |\lambda|}{\delta_n^2 + \gamma^2 / 4}, \quad (\text{B25})$$

which, stated differently, can be written as

$$L_n = n \times \left( \frac{c T_n}{2L} \right), \quad (\text{B26})$$

for the case of  $\phi = 0$  or  $\pi$ . This is Eq. (4) of the main text. Our model also considers more general coupling phases between the direct and indirect channels. Thus, the physical interpretation is evidently that the loss per photon ( $L_n/n$ ) is simply the round-trip rate of light propagation in the cavity, multiplied by the cavity transmission. This is largely what one intuitively expects, and is borne out from the density-matrix approach in the adiabatic approximation. This identification however, suggests a generalization to more complicated Fano mirrors, supporting perhaps multiple internal modes: the loss can be specified in terms of the experimental transmission as a function of frequency.

## 2. Langevin force description of a nonlinear resonator with loss

In this section, we develop a complementary perspective on the description of dissipation in a nonlinear resonator with sharply varying loss. In quantum optics, it is well-established that

there are two equivalent ways to formulate dissipation. The first approach is formulated through the density-matrix in the Born-Markov approximation, as developed in the previous section. The second is formulated through the Heisenberg equations of motion that resemble classical equations of damping, except with operator-valued forces added to the equations to ensure preservation of operator commutation relations at all times.

The methods are highly complementary to each other, and present definite advantages over the other. In the density matrix approach, the equations for the density matrix elements are linear, and it is possible to find the evolution of the density matrix elements in a conceptually straightforward way. The density matrix method is the one which is mostly used in modern quantum engineering, and we have thus made the density-matrix approach the primary method.

The Heisenberg-Langevin on the other hand, generally leads to nonlinear operator equations with quantum stochastic force terms that have no definite numerically implementable representation (though they may be mapped to classical stochastic differential equations). However, the main advantages of the Heisenberg approach emerge in situations where quantum fluctuations are small compared to the mean values (as is the case in every system we analyze in the main text). In that case, operator expectation values, even for macroscopic states of light (that cannot be numerically stored as a density matrix, due to sheer dimensionality), can be readily found through a small number of coupled linear differential equations. From a fundamental standpoint, the Heisenberg-Langevin approach also has the advantage of bearing close similarity to classical equations of motion. Very often, one may simply take classical equations, add stochastic force terms, and find the correlation functions of the forces through the Einstein relations [64, 65]. The Langevin approach has proven itself to be very useful in the context of laser physics for this reason. From the standpoint of lasers, it is also important because it turns out that for many important gain media, such as solid-state lasers and semiconductor lasers, one cannot eliminate the gain from the density matrix, and the density matrix then becomes too cumbersome to derive useful results. In those cases, the Langevin approach proves to be the only workable method. For all of these reasons, we now develop the Heisenberg-Langevin equations for the photon number operator.

We follow the general method for deriving Langevin equations for quantum systems presented in [66] (there, the method is applied to derive Langevin equations for a two-level system). In this method, one asserts the following Heisenberg-Langevin equations for the projectors:

$$\dot{T}_{n,n} = -L_n T_{n,n} + L_{n+1} T_{n+1,n+1} + F_{n,n}, \quad (\text{B27})$$

where  $F_{n,n}$  are operator valued forces associated with the effect of the reservoir (with operators  $b_k$  and  $d$ ) defined in Eq. (3). The force is assumed to have zero mean but finite second-order correlations that are delta-correlated (schematically  $\langle F(t)F(t') \rangle = 2D\delta(t-t')$  for some operator-valued “diffusion coefficient”  $D$ ). While at the level of Eq. (27), this appears as an assumption, it may also be shown directly by adding reservoir terms to the Heisenberg equation and integrating out the reservoirs in the Markov and adiabatic approximations. This is demonstrated in the final section. Note that Eq. (27) is “just” the corresponding operator equation to Eq. (22): taking the expectation value  $\text{tr}[\rho \dot{T}_{n,n}] = \dot{\rho}_{n,n}$  yields  $-L_n \rho_{n,n} + L_{n+1} \rho_{n+1,n+1}$  (using the fact that  $\langle F_{n,n} \rangle = 0$ ).

The correlation functions between different forces ( $F_\mu, F_\nu$ , corresponding to the equations of motion for operators  $A_\mu, A_\nu$ ) – provided they have zero mean and are delta-correlated in time (memory-less) – satisfy the so-called Einstein-relation for the diffusion coefficient  $D_{\mu\nu}$  satisfying  $\langle F_\mu(t)F_\nu(t') \rangle \equiv 2\langle D_{\mu\nu} \rangle \delta(t-t')$ :

$$2\langle D_{\mu\nu} \rangle = \frac{d}{dt} \langle A_\mu A_\nu \rangle - \langle A_\mu D_\nu \rangle - \langle D_\mu A_\nu \rangle, \quad (\text{B28})$$

where the drift term,  $D_\mu$  is defined such that  $\dot{A}_\mu = D_\mu + F_\mu$ . Applying this to Eq. (27) for example, we would say that for the operator  $T_{n,n}$ , the corresponding  $D_\mu$  is  $-L_n T_{n,n} + L_{n+1} T_{n+1,n+1}$  and the corresponding  $F_\mu$  is  $F_{n,n}$ .

Let us now use these relations to get an equation of motion for the photon number operator  $n = \sum_{j=0}^{\infty} j T_{j,j}$ , for which the corresponding Langevin force is  $F_n = \sum_j j F_{j,j}$ . The correlation function is then given by  $\langle F_n(t)F_n(t') \rangle = \sum_{j,k} jk \langle F_{j,j}(t)F_{k,k}(t') \rangle = \sum_{j,k} 2jk \langle D_{jj,kk} \rangle \delta(t-t')$ . The diffusion coefficient can be evaluated from the Einstein relation as:

$$2\langle D_{jj,kk} \rangle = \delta_{j,k} \langle \dot{T}_{j,j} \rangle - \langle T_{j,j} D_{k,k} \rangle - \langle D_{j,j} T_{k,k} \rangle, \quad (\text{B29})$$

where we have used that  $\langle T_{j,j} T_{k,k} \rangle = \delta_{jk} T_{j,k}$ . Plugging in the drift terms and evaluating the sum yields

$$\begin{aligned} 2\langle D_{n,n} \rangle &= \sum_{j,k=0}^{\infty} 2jk \langle D_{jj,kk} \rangle \\ &= \sum_{jk} 2jk \left( \delta_{j,k} \langle \dot{T}_{j,j} \rangle - \langle T_{j,j} (-L_k T_{k,k} + L_{k+1} T_{k+1,k+1}) \rangle - \langle (-L_j T_{j,j} + L_{j+1} T_{j+1,j+1}) T_{k,k} \rangle \right) \\ &= \sum_{j=0}^{\infty} \langle j(L_j T_{j,j} - L_{j+1} T_{j+1,j+1}) \rangle = \sum_{j=0}^{\infty} L_j \langle T_{j,j} \rangle = \langle L(n) \rangle = \langle n\kappa(n) \rangle, \end{aligned} \quad (\text{B30})$$

where we have used  $L_0 = 0$ . In the last two equalities,  $L(n) = n\kappa(n)$  is understood to be a function of the  $n$ -operator.

The drift term in the equation of motion for  $n$  can be evaluated by similar manipulations. It is given by

$$\sum_{j=0}^{\infty} j(L_{j+1}T_{j+1} - L_jT_j) = -\sum_{j=0}^{\infty} L_jT_j = L(n), \quad (\text{B31})$$

Putting it all together, we find that the Heisenberg-Langevin equation of motion for the photon number is

$$\dot{n} = -\kappa(n)n + F_n. \quad (\text{B32})$$

Eq. (32) is the main result of the Langevin theory of decay of an anharmonic oscillator with intensity-dependent loss of the type resulting from nonlinear dispersive loss introduced in Sec. II.

In the next section, we will use this Langevin equation, in conjunction with the known Langevin equations describing a pumped gain medium, to derive the quantum statistical theory of lasers with sharp intensity-dependent loss. We then show how Fock and macroscopic sub-Poissonian states result.

### Appendix C: Lasers based on sharp loss

In this section, we develop the core equations underpinning the theory of lasers with sharp intensity-dependent loss elements. The main question to answer is: what is the combined effect of a gain medium and sharp intensity-dependent loss on the transient and steady-state quantum statistics of the cavity mode? The answer to this question fundamentally depends on the properties of the gain medium. In particular, the answer depends on how the polarization and inversion decay times,  $\gamma_{\perp}, \gamma_{\parallel}$  compare to the cavity decay rate at equilibrium  $\kappa(n_0)$ , with  $n_0$  the steady-state photon number. In all cases, we will consider the case in which  $\gamma_{\perp} = T_2^{-1}$  is fast compared to the cavity decay time, as this is typically borne out for most gain media. On the other hand, the inversion decay  $\gamma_{\parallel} = T_1^{-1}$  can fall on either side of the cavity decay rate for important gain media. For solid-state lasers like Nd:YAG, the  $\gamma_{\parallel} < \kappa$  except in cases of cavities with extremely low amounts of loss. For molecular dyes and gas lasers,  $\gamma_{\parallel}$  is fast. For semiconductor lasers, where  $\gamma_{\parallel}^{-1} \sim 1$  ns, it depends on the cavity geometry (e.g., an external cavity constructed around the semiconductor gain chip would give the photon a long lifetime and lead to  $\kappa \ll \gamma_{\parallel}$ ). The two cases ( $\kappa \ll \gamma_{\parallel}$  and  $\kappa \gg \gamma_{\parallel}$ ) are often referred to as class-A and class-B regimes respectively. The class-A regime is significantly simpler to describe, and also leads in general to lower noise in the photon. The class-B regime introduces additional noise to the photon in the form of relaxation-oscillations, which

magnify the quantum fluctuations of the inversion, and lead to enhanced noise for the photon.

### 1. Quantum statistics of lasers with sharp loss for fast inversion lasers

Let us start by describing the class-A regime, which applies to lasers with rapidly-decaying or “fast” inversion. In this case, the gain medium can be eliminated from the joint gain-photon density matrix, leading to a single equation of motion for the photon. Because the photon state (which changes on the cavity time-scale) hardly changes over the time-scale  $\gamma_{||}, \gamma_{\perp}$ , one may simply find the effect of the gain medium on the photon density matrix ignoring the cavity loss, and then afterwards add terms associated with the loss (Eq. (22)). This procedure is very well-documented in the literature, and for a reader interested in the details, we refer them for example to the treatment of [17] (Chapter 11).

The combined effect of the gain-medium and the cavity loss on the equation of motion for the photon probabilities is

$$\dot{\rho}_{n,n} = G_n \rho_{n-1,n-1} - (G_{n+1} + L_n) \rho_{n,n} + L_{n+1} \rho_{n+1,n+1}, \quad (\text{C1})$$

where

$$G_n = \frac{An}{1 + n/n_s}, \quad (\text{C2})$$

with  $A$  being the linear gain coefficient and  $n_s$  being the saturation photon number. Here, we have assumed that the gain medium is resonant with the cavity. Few qualitative changes are introduced by including a finite detuning.

Let us find the steady-state photon statistics for a laser governed by these equations. Thus we want to solve  $\dot{\rho}_n = 0$  with the constraint  $\sum_n \rho_n = 1$  (introducing the shorthand  $\rho_n = \rho_{nn}$ ). Writing the steady-state equation as  $0 = G_n \rho_{n-1} + (-G_{n+1} + L_n) \rho_n + L_{n+1} \rho_{n+1}$ . This equation, which implies

$$G_n \rho_{n-1} - L_n \rho_n = G_{n+1} \rho_n - L_{n+1} \rho_{n+1}, \quad (\text{C3})$$

enables exact solution of the steady-state. Defining the difference  $S_n = G_n \rho_{n-1} - L_n \rho_n$ , we see that  $S_n = S_{n+1}$ . Since  $S_0 = G_0 \rho_{-1} - L_0 \rho_0 = 0$ , we have that  $S_n = 0$  for all  $n$ , and thus the simpler recursion relation:

$$\rho_{n+1} = \frac{G_{n+1}}{L_{n+1}} \rho_n \implies \rho_n = \frac{1}{Z} \left( \prod_{m=1}^n \frac{G_m}{L_m} \right) \rho_0, \quad (\text{C4})$$

with  $Z$  a normalization constant enforcing  $\sum_n \rho_n = 1$ .

## 2. Quantum statistics of lasers with sharp loss for slow inversion lasers

Let us now find the quantum statistics of a nonlinear laser with sharp loss in the case where the gain medium may have a slow inversion (the equations also apply in the case of fast inversion, and give identical statistical predictions as Eq. (33) in that case).

In the case of slow inversion, while the gain medium cannot be eliminated from the density matrix of the atom and photon, we may still describe the system by means of Langevin equations for the photon number ( $n$ ) and population inversion operators ( $S$ ). The dynamics are effectively given by rate equations, but with operator-valued Langevin forces [40]. In particular, the equations of motion are:

$$\begin{aligned}\dot{n} &= (R_{\text{sp}}S - \kappa(n))n + F_n \\ \dot{S} &= \Lambda - (\gamma_{\parallel} + R_{\text{sp}}n)S + F_S,\end{aligned}\tag{C5}$$

where  $R_{\text{sp}}$  is the rate of spontaneous emission into the cavity mode,  $\Lambda$  is the rate of pumping of the gain medium, and  $\gamma_{\parallel}$  is the inversion relaxation rate. Let us briefly comment on the terms in the Langevin equations. The dynamics of  $n$  are governed by the competition between stimulated emission and loss (which here, we take as being entirely due to radiative losses). The photons increase due to stimulated emission at rate  $R_{\text{sp}}Sn$ , with  $R_{\text{sp}}$  being the rate of spontaneous emission into the cavity mode. Beyond stimulated emission, the photon number also decreases due to cavity losses, at rate  $\kappa(n)n$ , with  $\kappa(n)$  the cavity leakage rate. Importantly, the cavity leakage rate is sharply photon-number dependent in the presence of nonlinearity. This is due to the fact that the complex frequency of the unloaded cavity changes when the index of refraction of the cavity changes. For example, in a cavity in which one of the mirrors has a frequency-dependent transmission  $T(\omega)$ , the leakage rate would be simply  $\frac{v_g}{2L}T(\omega(n))$  with  $v_g$  being the velocity of light in the cavity and  $L$  being the cavity length. In a similar fashion, the dynamics of the total inversion,  $S$  are governed by the competing forces of pumping and relaxation. The pumping occurs at rate  $\Lambda$ . Relaxation occurs due to non-lasing decays at rate  $\gamma_{\parallel}$ , as well as stimulated emission at rate  $R_{\text{sp}}(n)nS$ .

The terms  $F_n$  and  $F_S$  are operator-valued Langevin forces which lead to non-deterministic dynamics of the photon number and inversion. In the absence of these forces, the photon number and inversion would have a finite mean and zero uncertainty. In other words, it is due to these forces that there is any noise at all. These forces have zero mean, and correlation functions given

by  $\langle F_i(t)F_j(t') \rangle = \langle 2D_{ij} \rangle \delta(t - t')$  with  $i, j = n, S$ . The diffusion coefficients,  $2D_{ij}$  are given by:

$$\begin{aligned} 2D_{nn} &= \langle (R_{\text{sp}}S + \kappa(n)) n \rangle \\ 2D_{nS} &= 2D_{Sn} = -\langle R_{\text{sp}}Sn \rangle \\ 2D_{SS} &= \Lambda + \langle (\gamma_{||} + R_{\text{sp}}n) S \rangle. \end{aligned} \quad (\text{C6})$$

With the terms in the Langevin equations described, let us now solve for the photon statistics. We are primarily interested in the cavity photon statistics at the steady-state operating point of the laser. We will quantify the photon statistics primarily by the mean and variance of the cavity photon number (a variance of zero would correspond to a cavity Fock state). In all cases we consider in this paper (even the noisiest ones), the quantum fluctuations of the photon number and inversion are small compared to the mean values. Thus, we may linearize the Langevin equations (which are nonlinear in  $n$  and  $S$ ) around their mean values as:  $n = \bar{n} + \delta n$  and  $S = \bar{S} + \delta S$ . The quantities  $\bar{n}$  and  $\bar{S}$  are c-number (mean) values, while  $\delta n$  and  $\delta S$  are operator-valued fluctuations. It follows immediately from the definitions above, and the zero-mean values of the forces, that  $\langle n \rangle = \bar{n}$  and  $\delta n = \langle \delta n \rangle$ . These fluctuations are of the same order as the Langevin forces  $F_n$  and  $F_S$ . The resulting linearized equations can be solved order-by-order to find the mean value and variance of the photon number and inversion.

The mean values of the inversion follows from the linearized equations as  $\bar{S} = \frac{\Lambda}{\gamma_{||} + R_{\text{sp}}(\bar{n})}$ . The mean value of the photon number then satisfies:

$$\frac{R_{\text{sp}}\Lambda}{\gamma_{||} + R_{\text{sp}}\bar{n}} = \kappa(\bar{n}), \quad (\text{C7})$$

which expresses the expected fact that at the steady-state, the saturated balances the (nonlinear) loss. In the absence of nonlinear loss ( $R_{\text{sp}}(\bar{n}) \rightarrow R_{\text{sp}}$  and  $\kappa(\bar{n}) \rightarrow \kappa$ ), this solution of this equations coincides completely with the expected number of photons in a single-mode laser cavity at its steady-state. In the presence of significant nonlinear loss, the equation becomes a nonlinear equation for the photon number that may admit multiple solutions, and also has a nonlinear dependence on the pump rate. Now let us move to find the fluctuations.

The fluctuations of the photon number and inversion satisfy the pair of coupled equations

$$\begin{pmatrix} \dot{\delta n} \\ \dot{\delta S} \end{pmatrix} = \begin{pmatrix} (-\kappa'(\bar{n})\bar{n} & R_{\text{sp}}\bar{n} \\ -R_{\text{sp}}\bar{S} & -(\gamma_{||} + R_{\text{sp}}\bar{n}) \end{pmatrix} \begin{pmatrix} \delta n \\ \delta S \end{pmatrix} + \begin{pmatrix} F_n \\ F_S \end{pmatrix}. \quad (\text{C8})$$

Here, we have introduced  $\kappa'(n) = d\kappa/dn$ . These terms quantify the sharpness of the loss. This pair of linear equations may be expressed simply as  $\delta\dot{V} = M\delta V + F$  with  $\delta V = (\delta n, \delta S)^T$ ,  $F =$

$(F_n, F_S)^T$ , and  $M$  the matrix in Equation (40). Fourier transforming, one obtains:  $-i\omega\delta V(\omega) = M\delta V(\omega) + F(\omega)$  which yields the solution  $\delta V(\omega) = -[M + i\omega]^{-1}F(\omega) \equiv K(\omega)F(\omega)$ . The photon number uncertainty is given simply by integrating over the amplitude noise spectrum  $S_{nn}(\omega)$ , defined by:

$$(\Delta n)^2 = \int_0^\infty d\omega S_{nn}(\omega) \equiv \frac{1}{\pi} \int_0^\infty d\omega \langle \delta n^\dagger(\omega) \delta n(\omega) \rangle. \quad (\text{C9})$$

The noise spectrum may analytically be derived from Eq. (40). The result is:

$$S_{nn}(\omega) = \frac{1}{\pi} \frac{n(2\kappa(\gamma^2 + \omega^2) + \kappa n^2 R^2 + nR(3\gamma\kappa + \Lambda R))}{(\omega^4 + \omega^2(\kappa'^2 n^2 + (\gamma + nR)^2 - 2\kappa nR) + n^2(\kappa'(\gamma + nR) + \kappa R)^2)}, \quad (\text{C10})$$

of which examples are plotted in Fig. 5 of the main text for the case of an Nd:YAG laser with a sharp transmissive element.

#### **Appendix D: Deriving the effect of nonlinear loss on probabilities and coherences directly from the Heisenberg picture**

In Section S2 (“Quantum theory of a nonlinear resonator with frequency-dependent loss”), we derived the equation of motion for the photon probabilities from a reservoir theory in which we considered the joint coupling of the cavity and end-mirror to the resonator. We derived a master equation for the density matrix of the cavity and mirror and we then adiabatically eliminated the end mirror. We now provide a potentially simpler and more direct derivation of the result from the Heisenberg equations of motion. This derivation fully agrees with our findings from the density matrix.

##### **1. General framework**

Our goal will be to derive a set of Heisenberg equations of motion to describe the photon in the nonlinear cavity. In a conventional laser theory based on Langevin equations, one writes an equation of motion for  $a$ . For the nonlinear laser considered here, this approach is complicated by the polychromatic nature of a nonlinear oscillator. In particular, the operator  $a$  can be expressed as  $a = \sum_n \sqrt{n} |n-1\rangle \langle n| \equiv \sum_n \sqrt{n} T_{n-1,n}$ . In the absence of interactions with gain or reservoirs, the time-evolution of  $a$  would simply be  $a(t) = \sum_n \sqrt{n} T_{n-1,n}(0) e^{-i\omega_{n,n-1}t}$  with  $\omega_{n,n-1} = \omega_n - \omega_{n-1}$ . For a linear photon,  $\omega_{n,n-1} = n\omega - (n-1)\omega = \omega$ , independently of  $n$ , recovering the familiar monochromatic evolution  $a(t) = a(0)e^{-i\omega t}$ .



While the polychromatic nature of  $a$  evades solution by conventional methods, the time evolution of the operators  $T_{n-1,n}$ , and more generally,  $T_{n-k,n}$ , is quite simple. For example, in the absence of gain or loss, the time-evolution of the operator  $T_{n-k,n}$  is given as:

$$\dot{T}_{n-k,n} = \frac{i}{\hbar} \left[ \sum_m \hbar \omega_m T_{m,m}, T_{n-k,n} \right] = -i \omega_{n,n-k} T_{n-k,n}, \quad (\text{D1})$$

so that  $T_{n-k,n}(t) = T_{n-k,n}(0)e^{-i\omega_{n,n-k}t}$ . Thus, the operators  $T_{n-k,n}$  have a simple monochromatic evolution in the absence of interactions. The simplicity of the equation of motion for the projectors then motivates us to formulate our quantum theory of nonlinear loss through the equations of motion for the  $T_{n-k,n}$ , for each  $k$ . Each  $k$  corresponds to a quantity with clear physical significance. The case of  $k = 0$ , which is of primary interest in this work, corresponds to probabilities/populations. In particular,  $\langle T_{n,n} \rangle = \text{tr}[\rho T_{n,n}]$  corresponds to the probability of having  $n$  photons. The case of  $k$  finite correspond to coherences, with  $\langle T_{n-1,n} \rangle$  corresponding to first-order (phase) coherence (and the laser linewidth) and  $\langle T_{n-2,n} \rangle$  corresponding to second-order (intensity) coherence.

In deriving Eq. (43), we have made use of the fundamental identity of projectors  $T_{ij}T_{kl} = \delta_{jk}T_{il}$ . We will make heavy use of this identity throughout this section. Beyond this, the following two identities are also used frequently:

$$[a, T_{n-k,n}] = \sqrt{n-k}T_{n-k-1,n} - \sqrt{n+1}T_{n-k,n+1}, \quad (\text{D2})$$

$$[a^\dagger, T_{n-k,n}] = \sqrt{n-k+1}T_{n-k+1,n} - \sqrt{n}T_{n-k,n-1}. \quad (\text{D3})$$

We have already found the contribution of free evolution to the equation of motion for  $T_{n-k,n}$ . Now we move to find the contribution from the sharp loss provided by the end mirror.

## 2. Loss terms

Now, we derive the contribution of cavity losses to the equation of motion for the  $k$ th coherences: defined as  $\dot{T}_{n-k,n}^{(\text{loss})}$ . We have

$$\begin{aligned}
\dot{T}_{n-k,n}^{(\text{loss})} &= i \left[ (\lambda a d^\dagger + \lambda^* a^\dagger d) + \sum_k g_k (a b_k^\dagger + a^\dagger b_k), T_{n-k,n} \right] \\
&= i \sum_k g_k b_k^\dagger (\sqrt{n-k} T_{n-k-1,n} - \sqrt{n+1} T_{n-k,n+1}) + i \sum_k g_k (\sqrt{n-k+1} T_{n-k+1,n} - \sqrt{n} T_{n-k,n-1}) b_k \\
&\quad + i \lambda d^\dagger (\sqrt{n-k} T_{n-k-1,n} - \sqrt{n+1} T_{n-k,n+1}) + i \lambda^* (\sqrt{n-k+1} T_{n-k+1,n} - \sqrt{n} T_{n-k,n-1}) d \\
&\equiv (\text{L1A}) + (\text{L1B}) + (\text{L2A}) + (\text{L2B}). \tag{D4}
\end{aligned}$$

The labels L1A, L1B, L2A, and L2B have been introduced for convenience. Here, we have normally ordered the reservoir operators, as we will exclusively consider initial conditions involving no excitations in the far-field or the internal mode of the Fano mirror. Therefore, upon taking expectation values, terms involving the initial values of these operators (Langevin forces) will vanish.

To proceed, we must eliminate the reservoirs from the equations. This is done through the Heisenberg equations of motion for the far-field reservoir and the internal mode of the Fano mirror. The equation for  $b_k$  reads:

$$\dot{b}_k = -i\omega_k b_k - i g_k a - i v_k d, \tag{D5}$$

admitting the formal solution

$$b_k(t) = b_k(0) e^{-i\omega_k t} - i \int_0^t dt' (g_k a(t') + v_k d(t')) e^{-i\omega_k(t-t')}. \tag{D6}$$

Meanwhile, the equation for  $d$  reads

$$\dot{d} = -i\omega_d d - i\lambda a - i \sum_k v_k b_k. \tag{D7}$$

To proceed, let us eliminate  $b$  from the equation of motion for  $d$ . This yields:

$$\dot{d} = -i\omega_d d - i\lambda a - i \sum_k v_k \left( b_k(0) e^{-i\omega_k t} - i \int_0^t dt' (g_k a(t') + v_k d(t')) e^{-i\omega_k(t-t')} \right). \tag{D8}$$

To proceed, we make note of the fact that in laser theory, the coupling between cavity modes and the far-field is well-approximated as a white noise coupling which is independent of frequency, so

that  $g_k = g$  and  $v_k = v$  (Markov approximation). In that case, the sum over  $k$  can be carried out. In the continuum limit,  $\sum_k \rightarrow \int d\omega_k \rho$ , with  $\rho$  the (constant) density of (far-field) states, and the sum yields

$$\dot{d} = -is_d d - G_- a + F_d. \quad (\text{D9})$$

Here, we have used  $\int dt' \delta(t-t') f(t') = \frac{1}{2} f(t)$  and defined  $\gamma = 2\pi\rho v^2$ ,  $\kappa = 2\pi\rho g^2$ ,  $s_d = \omega_d - i\frac{\gamma}{2}$ , and  $G_- = i\lambda + \frac{1}{2}\sqrt{\kappa\gamma}$ . We have also defined the Langevin force on  $d$  via  $F_d = -i \sum_k v_k b_k(0) e^{-i\omega_k t}$ . We may now write the formal solution for  $d$  as

$$d(t) = d(0) e^{-is_d t} + \int_0^t dt' (-G_- a(t') + F_d(t')) e^{-is_d(t-t')}. \quad (\text{D10})$$

With the formal solutions for  $b$  and  $d$ , we may now plug them back into the terms L1A, L1B, L2A, and L2B. Let us start with L1A and L1B. L1A, under the Markov approximation, is given as:

$$(\text{L1A}) = \left( i \sum_k g_k b_k^\dagger(0) e^{i\omega_k t} - \frac{1}{2} (\kappa a^\dagger + \sqrt{\kappa\gamma} d^\dagger) \right) (\sqrt{n-k} T_{n-k-1,n} - \sqrt{n+1} T_{n-k,n+1}). \quad (\text{D11})$$

To proceed, we carry out the following steps (these will be repeated for the terms L1B, L2A, and L2B):

$$\begin{aligned} (\text{L1A}) = & \left( i \sum_k g_k b_k^\dagger(0) e^{i\omega_k t} \right) (\sqrt{n-k} T_{n-k-1,n} - \sqrt{n+1} T_{n-k,n+1}) \\ & - \frac{1}{2} \kappa ((n-k) T_{n-k,n} - \sqrt{(n+1)(n-k+1)} T_{n-k+1,n+1}) \\ & + \frac{1}{2} \sqrt{\kappa\gamma} \int_0^t dt' G_-^* a^\dagger(t') e^{is_d^*(t-t')} (\sqrt{n-k} T_{n-k-1,n} - \sqrt{n+1} T_{n-k,n+1}) \\ & - \frac{1}{2} \sqrt{\kappa\gamma} \left( d^\dagger(0) e^{is_d^* t} + \int_0^t dt' F_d^\dagger(t') e^{is_d^*(t-t')} \right) (\sqrt{n-k} T_{n-k-1,n} - \sqrt{n+1} T_{n-k,n+1}). \end{aligned} \quad (\text{D12})$$

In what follows, we consider the limiting case in which the decay of  $d$ , set by  $\gamma$  is much faster than the gain dynamics. This is the same adiabatic approximation that was used to simplify the equation of motion for the gain. Under those conditions, the third term becomes:

$$\frac{1}{2} \sqrt{\kappa\gamma} G_-^* \left( \frac{n-k}{i(\omega_{n-k,n-k-1} - s_d^*)} T_{n-k,n} - \frac{\sqrt{(n+1)(n-k+1)}}{i(\omega_{n-k+1,n-k} - s_d^*)} T_{n-k+1,n+1} \right). \quad (\text{D13})$$

This allows us to write L1A as

$$\begin{aligned}
(\text{L1A}) = & -\frac{1}{2}\kappa((n-k)T_{n-k,n} - \sqrt{(n+1)(n-k+1)}T_{n-k+1,n+1}) \\
& + \frac{1}{2}\sqrt{\kappa\gamma}G_-^* \left( \frac{n-k}{i(\omega_{n-k,n-k-1} - s_d^*)}T_{n-k,n} - \frac{\sqrt{(n+1)(n-k+1)}}{i(\omega_{n-k+1,n-k} - s_d^*)}T_{n-k+1,n+1} \right) \\
& + \left( i \sum_k g_k b_k^\dagger(0) e^{i\omega_k t} \right) (\sqrt{n-k}T_{n-k-1,n} - \sqrt{n+1}T_{n-k,n+1}) \\
& - \frac{1}{2}\sqrt{\kappa\gamma} \left( d^\dagger(0)e^{is_d^*t} + \int_0^t dt' F_d^\dagger(t') e^{is_d^*(t-t')} \right) (\sqrt{n-k}T_{n-k-1,n} - \sqrt{n+1}T_{n-k,n+1}).
\end{aligned} \tag{D14}$$

As can be seen, the first two lines, upon taking expectation values, give terms of a similar form to the gain terms derived in the previous subsection. The remaining lines give zero expectation value when starting in the vacuum of the internal mode and the reservoir, and thus vanish when considering equations of motion for coherences.

Now, let us consider the remaining terms. L1B is quite similar to L1A, and we write

$$(\text{L1B}) = (\sqrt{n-k+1}T_{n-k+1,n} - \sqrt{n}T_{n-k,n-1}) \left( i \sum_k g_k b_k(0) e^{-i\omega_k t} + \frac{1}{2}(\kappa a + \sqrt{\kappa\gamma}d) \right), \tag{D15}$$

which may be further simplified as

$$\begin{aligned}
(\text{L1B}) = & \frac{1}{2}\kappa(\sqrt{(n-k+1)(n+1)}T_{n-k+1,n+1} - nT_{n-k,n}) \\
& - \frac{1}{2}\sqrt{\kappa\gamma}G_- \left( \frac{\sqrt{(n-k+1)(n+1)}}{i(s_d - \omega_{n+1,n})}T_{n-k+1,n+1} - \frac{n}{i(s_d - \omega_{n,n-1})}T_{n-k,n} \right) \\
& + (\sqrt{n-k+1}T_{n-k+1,n} - \sqrt{n}T_{n-k,n-1}) \left( i \sum_k g_k b_k(0) e^{-i\omega_k t} \right) \\
& + \frac{1}{2}\sqrt{\kappa\gamma}(\sqrt{n-k+1}T_{n-k+1,n} - \sqrt{n}T_{n-k,n-1}) \left( d(0)e^{-is_d t} + \int_0^t dt' F_d(t') e^{-is_d(t-t')} \right),
\end{aligned} \tag{D16}$$

where we have taken all the same steps as those leading to Eq. (56).

The term L2A is given as:

$$(\text{L2A}) = i\lambda \left( d^\dagger(0)e^{is_d^*t} + \int_0^t dt' \left( -G_-^* a^\dagger(t') + F_d^\dagger(t') \right) e^{+is_d^*(t-t')} \right) (\sqrt{n-k}T_{n-k-1,n} - \sqrt{n+1}T_{n-k,n+1}). \tag{D17}$$

Under the adiabatic approximation, we may then write:

$$\begin{aligned}
(\text{L2A}) = & -i\lambda G_-^* \left( \frac{(n-k)}{i(\omega_{n-k,n-k-1} - s_d^*)} T_{n-k,n} - \frac{\sqrt{(n-k+1)(n+1)}}{i(\omega_{n-k+1,n-k} - s_d^*)} T_{n-k+1,n+1} \right) \\
& + i\lambda \left( d^\dagger(0) e^{is_d^* t} + \int_0^t dt' F_d^\dagger(t') e^{+is_d^*(t-t')} \right) (\sqrt{n-k} T_{n-k-1,n} - \sqrt{n+1} T_{n-k,n+1}).
\end{aligned} \tag{D18}$$

The term L2B:

$$(\text{L2B}) = i\lambda^* (\sqrt{n-k+1} T_{n-k+1,n} - \sqrt{n} T_{n-k,n-1}) \left( d(0) e^{-is_d t} + \int_0^t dt' (-G_- a(t') + F_d(t')) e^{-is_d(t-t')} \right), \tag{D19}$$

similarly follows as:

$$\begin{aligned}
(\text{L2B}) = & -i\lambda^* G_- \left( \frac{\sqrt{(n-k+1)(n+1)}}{i(s_d - \omega_{n+1,n})} T_{n-k+1,n+1} - \frac{n}{i(s_d - \omega_{n,n-1})} T_{n-k,n} \right) \\
& + i\lambda^* (\sqrt{n-k+1} T_{n-k+1,n} - \sqrt{n} T_{n-k,n-1}) \left( d(0) e^{-is_d t} + \int_0^t dt' F_d(t') e^{-is_d(t-t')} \right).
\end{aligned} \tag{D20}$$

Plugging L1A, L1B, L2A, and L2B into the equation for  $\dot{T}_{n-k,n}^{(\text{loss})}$ , we have

$$\begin{aligned}
\dot{T}_{n-k,n}^{(\text{loss})} = & \left( -\frac{1}{2} \kappa (2n-k) + \frac{(n-k) (-i\lambda + \frac{1}{2} \sqrt{\kappa\gamma}) G_-^*}{i(\omega_{n-k,n-k-1} - s_d^*)} - \frac{n (-i\lambda^* - \frac{1}{2} \sqrt{\kappa\gamma}) G_-}{i(s_d - \omega_{n,n-1})} \right) T_{n-k,n} \\
& + \sqrt{(n-k+1)(n+1)} \left( \kappa - \frac{(-i\lambda + \frac{1}{2} \sqrt{\kappa\gamma}) G_-^*}{i(\omega_{n-k+1,n-k} - s_d^*)} + \frac{(-i\lambda^* - \frac{1}{2} \sqrt{\kappa\gamma}) G_-}{i(s_d - \omega_{n+1,n})} \right) T_{n-k+1,n+1} \\
& + F_{n-k,n}^{(\text{loss})},
\end{aligned} \tag{D21}$$

The Langevin force  $F_{n-k,n}^{(\text{loss})}$  is given by

$$\begin{aligned}
F_{n-k,n}^{(\text{loss})} = & \left( i \sum_k g_k b_k^\dagger(0) e^{i\omega_k t} \right) (\sqrt{n-k} T_{n-k-1,n} - \sqrt{n+1} T_{n-k,n+1}) \\
& + (\sqrt{n-k+1} T_{n-k+1,n} - \sqrt{n} T_{n-k,n-1}) \left( i \sum_k g_k b_k(0) e^{-i\omega_k t} \right) \\
& + \left( i\lambda - \frac{1}{2} \sqrt{\kappa\gamma} \right) \left( d^\dagger(0) e^{is_d^* t} + \int_0^t dt' F_d^\dagger(t') e^{is_d^*(t-t')} \right) (\sqrt{n-k} T_{n-k-1,n} - \sqrt{n+1} T_{n-k,n+1}) \\
& + \left( i\lambda^* + \frac{1}{2} \sqrt{\kappa\gamma} \right) (\sqrt{n-k+1} T_{n-k+1,n} - \sqrt{n} T_{n-k,n-1}) \left( d(0) e^{-is_d t} + \int_0^t dt' F_d(t') e^{-is_d(t-t')} \right),
\end{aligned} \tag{D22}$$

and has the important property that  $\langle F_{n-k,n}^{(\text{loss})} \rangle = 0$  when the initial state is the vacuum of the reservoirs and the internal mode. Hence, for the systems we will consider here, such terms can be functionally ignored.

### 3. Equation of motion for the $k$ -th coherences

Here, we summarize the previous two sections, writing down the total equations of motion for the photon. The equation of motion for the  $k$ th coherences are

$$\begin{aligned}
\dot{T}_{n-k,n} = & -i\omega_{n,n-k} T_{n-k,n} \\
& + \left( -\frac{1}{2} \kappa(2n-k) + \frac{(n-k)(G_+ G_-)^*}{i(\omega_{n-k,n-k-1} - s_d^*)} + \frac{n G_+ G_-}{i(s_d - \omega_{n,n-1})} \right) T_{n-k,n} \\
& + \sqrt{(n-k+1)(n+1)} \left( \kappa - \frac{(G_+ G_-)^*}{i(\omega_{n-k+1,n-k} - s_d^*)} + \frac{G_+ G_-}{i(s_d - \omega_{n+1,n})} \right) T_{n-k+1,n+1} \\
& + F_{n-k,n}^{(\text{loss})},
\end{aligned} \tag{D23}$$

where

$$\begin{aligned}
F_{n-k,n}^{(\text{loss})} = & \left( i \sum_k g_k b_k^\dagger(0) e^{i\omega_k t} \right) (\sqrt{n-k} T_{n-k-1,n} - \sqrt{n+1} T_{n-k,n+1}) \\
& + (\sqrt{n-k+1} T_{n-k+1,n} - \sqrt{n} T_{n-k,n-1}) \left( i \sum_k g_k b_k(0) e^{-i\omega_k t} \right) \\
& + \left( i\lambda - \frac{1}{2} \sqrt{\kappa\gamma} \right) \left( d^\dagger(0) e^{is_d^* t} + \int_0^t dt' F_d^\dagger(t') e^{is_d^*(t-t')} \right) (\sqrt{n-k} T_{n-k-1,n} - \sqrt{n+1} T_{n-k,n+1}) \\
& + \left( i\lambda^* + \frac{1}{2} \sqrt{\kappa\gamma} \right) (\sqrt{n-k+1} T_{n-k+1,n} - \sqrt{n} T_{n-k,n-1}) \left( d(0) e^{-is_d t} + \int_0^t dt' F_d(t') e^{-is_d(t-t')} \right).
\end{aligned} \tag{D24}$$

One immediately sees that for  $k = 0$ , these equations are identical to those from the density matrix description – modulo the explicit form of the Langevin terms here, which resulted from our explicit account of the reservoir in the Heisenberg equations.

- 
- [1] Daniel F Walls. Squeezed states of light. *nature*, 306(5939):141–146, 1983.
  - [2] AI Lvovsky, Philippe Grangier, Alexei Ourjoumtsev, Valentina Parigi, Masahide Sasaki, and Rosa Tualle-Brouiri. Production and applications of non-gaussian quantum states of light. *arXiv preprint arXiv:2006.16985*, 2020.
  - [3] Robert Raussendorf, Daniel E Browne, and Hans J Briegel. Measurement-based quantum computation on cluster states. *Physical review A*, 68(2):022312, 2003.
  - [4] Nicolas C Menicucci, Peter Van Loock, Mile Gu, Christian Weedbrook, Timothy C Ralph, and Michael A Nielsen. Universal quantum computation with continuous-variable cluster states. *Physical review letters*, 97(11):110501, 2006.
  - [5] Christian Reimer, Stefania Sciara, Piotr Roztock, Mehedi Islam, Luis Romero Cortés, Yanbing Zhang, Bennet Fischer, Sébastien Loranger, Raman Kashyap, Alfonso Cino, et al. High-dimensional one-way quantum processing implemented on d-level cluster states. *Nature Physics*, 15(2):148–153, 2019.
  - [6] Mikkel V Larsen, Xueshi Guo, Casper R Breum, Jonas S Neergaard-Nielsen, and Ulrik L Andersen. Deterministic generation of a two-dimensional cluster state. *Science*, 366(6463):369–372, 2019.
  - [7] Malvin C Teich and Bahaa EA Saleh. Squeezed state of light. *Quantum Optics: Journal of the European Optical Society Part B*, 1(2):153, 1989.

- [8] Luiz Davidovich. Sub-poissonian processes in quantum optics. *Reviews of Modern Physics*, 68(1):127, 1996.
- [9] Nicholas Thomas-Peter, Brian J Smith, Animesh Datta, Lijian Zhang, Uwe Dorner, and Ian A Walm-  
sley. Real-world quantum sensors: evaluating resources for precision measurement. *Physical review  
letters*, 107(11):113603, 2011.
- [10] Scott Aaronson and Alex Arkhipov. The computational complexity of linear optics. In *Proceedings  
of the forty-third annual ACM symposium on Theory of computing*, pages 333–342, 2011.
- [11] Austin P Lund, Anthony Laing, Saleh Rahimi-Keshari, Terry Rudolph, Jeremy L O’Brien, and Timo-  
thy C Ralph. Boson sampling from a gaussian state. *Physical review letters*, 113(10):100502, 2014.
- [12] Joonsuk Huh, Gian Giacomo Guerreschi, Borja Peropadre, Jarrod R McClean, and Alán Aspuru-  
Guzik. Boson sampling for molecular vibronic spectra. *Nature Photonics*, 9(9):615–620, 2015.
- [13] Hui Wang, Yu He, Yu-Huai Li, Zu-En Su, Bo Li, He-Liang Huang, Xing Ding, Ming-Cheng  
Chen, Chang Liu, Jian Qin, et al. High-efficiency multiphoton boson sampling. *Nature Photonics*,  
11(6):361–365, 2017.
- [14] Craig S Hamilton, Regina Kruse, Linda Sansoni, Sonja Barkhofen, Christine Silberhorn, and Igor Jex.  
Gaussian boson sampling. *Physical review letters*, 119(17):170501, 2017.
- [15] Daniel J Brod, Ernesto F Galvão, Andrea Crespi, Roberto Osellame, Nicolò Spagnolo, and Fabio  
Sciarrino. Photonic implementation of boson sampling: a review. *Advanced Photonics*, 1(3):034001,  
2019.
- [16] Han-Sen Zhong, Hui Wang, Yu-Hao Deng, Ming-Cheng Chen, Li-Chao Peng, Yi-Han Luo, Jian Qin,  
Dian Wu, Xing Ding, Yi Hu, et al. Quantum computational advantage using photons. *Science*,  
370(6523):1460–1463, 2020.
- [17] Marlan O Scully and M Suhail Zubairy. Quantum optics, 1999.
- [18] Max Hofheinz, EM Weig, M Ansmann, Radoslaw C Bialczak, Erik Lucero, M Neeley, AD O’connell,  
H Wang, John M Martinis, and AN Cleland. Generation of fock states in a superconducting quantum  
circuit. *Nature*, 454(7202):310–314, 2008.
- [19] H Wang, M Hofheinz, M Ansmann, RC Bialczak, E Lucero, M Neeley, AD O’connell, D Sank,  
J Wenner, AN Cleland, et al. Measurement of the decay of fock states in a superconducting quantum  
circuit. *Physical Review Letters*, 101(24):240401, 2008.
- [20] Christopher S Wang, Jacob C Curtis, Brian J Lester, Yaxing Zhang, Yvonne Y Gao, Jessica Freeze,  
Victor S Batista, Patrick H Vaccaro, Isaac L Chuang, Luigi Frunzio, et al. Efficient multiphoton



- sampling of molecular vibronic spectra on a superconducting bosonic processor. *Physical Review X*, 10(2):021060, 2020.
- [21] Gerhard Rempe, F Schmidt-Kaler, and Herbert Walther. Observation of sub-poissonian photon statistics in a micromaser. *Physical review letters*, 64(23):2783, 1990.
  - [22] Benjamin TH Varcoe, Simon Brattke, Matthias Weidinger, and Herbert Walther. Preparing pure photon number states of the radiation field. *Nature*, 403(6771):743–746, 2000.
  - [23] Clément Sayrin, Igor Dotsenko, Xingxing Zhou, Bruno Peaudecerf, Théo Rybarczyk, Sébastien Gleyzes, Pierre Rouchon, Mazyar Mirrahimi, Hadis Amini, Michel Brune, et al. Real-time quantum feedback prepares and stabilizes photon number states. *Nature*, 477(7362):73–77, 2011.
  - [24] Edo Waks, Eleni Diamanti, Barry C Sanders, Stephen D Bartlett, and Yoshihisa Yamamoto. Direct observation of nonclassical photon statistics in parametric down-conversion. *Physical review letters*, 92(11):113602, 2004.
  - [25] Merlin Cooper, Laura J Wright, Christoph Söller, and Brian J Smith. Experimental generation of multi-photon fock states. *Optics express*, 21(5):5309–5317, 2013.
  - [26] M Kitagawa and Y Yamamoto. Number-phase minimum-uncertainty state with reduced number uncertainty in a kerr nonlinear interferometer. *Physical Review A*, 34(5):3974, 1986.
  - [27] Daniel F Walls and Gerard J Milburn. *Quantum optics*. Springer Science & Business Media, 2007.
  - [28] PD Drummond and DF Walls. Quantum theory of optical bistability. i. nonlinear polarisability model. *Journal of Physics A: Mathematical and General*, 13(2):725, 1980.
  - [29] Robert W Boyd. *Nonlinear optics*. Academic press, 2020.
  - [30] Hermann Haus. Waves and fields in optoelectronics. *Prentice-Hall, Inc.*, 1984.
  - [31] Mehmet Fatih Yanik, Shanhui Fan, and Marin Soljačić. High-contrast all-optical bistable switching in photonic crystal microcavities. *Applied Physics Letters*, 83(14):2739–2741, 2003.
  - [32] Thomas Fink, Anne Schade, Sven Höfling, Christian Schneider, and Ataç Imamoglu. Signatures of a dissipative phase transition in photon correlation measurements. *Nature Physics*, 14(4):365–369, 2018.
  - [33] A Imamoglu, Helmut Schmidt, Gareth Woods, and Moshe Deutsch. Strongly interacting photons in a nonlinear cavity. *Physical Review Letters*, 79(8):1467, 1997.
  - [34] Aymeric Delteil, Thomas Fink, Anne Schade, Sven Höfling, Christian Schneider, and Ataç İmamoglu. Towards polariton blockade of confined exciton–polaritons. *Nature materials*, 18(3):219–222, 2019.
  - [35] Nicholas Rivera and Ido Kaminer. Light–matter interactions with photonic quasiparticles. *Nature*

- Reviews Physics*, 2(10):538–561, 2020.
- [36] François Bondu, P Fritschel, CN Man, and A Brillet. Ultrahigh-spectral-purity laser for the virgo experiment. *Optics letters*, 21(8):582–584, 1996.
  - [37] Marlan O Scully and Willis E Lamb Jr. Quantum theory of an optical maser. i. general theory. *Physical Review*, 159(2):208, 1967.
  - [38] Shanhui Fan and John D Joannopoulos. Analysis of guided resonances in photonic crystal slabs. *Physical Review B*, 65(23):235112, 2002.
  - [39] Shanhui Fan, Wonjoo Suh, and John D Joannopoulos. Temporal coupled-mode theory for the fano resonance in optical resonators. *JOSA A*, 20(3):569–572, 2003.
  - [40] Melvin Lax. Quantum noise vii: The rate equations and amplitude noise in lasers. *IEEE Journal of Quantum Electronics*, 3(2):37–46, 1967.
  - [41] Y Yamamoto, S Machida, and O Nilsson. Amplitude squeezing in a pump-noise-suppressed laser oscillator. *Physical Review A*, 34(5):4025, 1986.
  - [42] S Machida and Y Yamamoto. Observation of sub-poissonian photoelectron statistics in a negative feedback semiconductor laser. *Optics communications*, 57(4):290–296, 1986.
  - [43] WH Richardson, S Machida, and Y Yamamoto. Squeezed photon-number noise and sub-poissonian electrical partition noise in a semiconductor laser. *Physical review letters*, 66(22):2867, 1991.
  - [44] Yoshihisa Yamamoto, Susumu Machida, and Wayne H Richardson. Photon number squeezed states in semiconductor lasers. *Science*, 255(5049):1219–1224, 1992.
  - [45] H Ritsch. Quantum noise reduction in lasers with nonlinear absorbers. *Quantum Optics: Journal of the European Optical Society Part B*, 2(2):189, 1990.
  - [46] DANIEL F Walls, MJ Collett, and AS Lane. Amplitude-noise reduction in lasers with intracavity nonlinear elements. *Physical Review A*, 42(7):4366, 1990.
  - [47] Seema Lathi and Yoshihisa Yamamoto. Influence of nonlinear gain and loss on the intensity noise of a multimode semiconductor laser. *Physical Review A*, 59(1):819, 1999.
  - [48] VSC Canela and HJ Carmichael. Bright sub-poissonian light through intrinsic feedback and external control. *Physical review letters*, 124(6):063604, 2020.
  - [49] HM Wiseman and GJ Milburn. Noise reduction in a laser by nonlinear damping. *Physical Review A*, 44(11):7815, 1991.
  - [50] H Ritsch, MAM Marte, and P Zoller. Quantum noise reduction in raman lasers. *EPL (Europhysics Letters)*, 19(1):7, 1992.

- [51] Amnon Yariv, Rashit Nabiev, and Kerry Vahala. Self-quenching of fundamental phase and amplitude noise in semiconductor lasers with dispersive loss. *Optics letters*, 15(23):1359–1361, 1990.
- [52] J Kitching, R Boyd, A Yariv, and Y Shevy. Amplitude noise reduction in semiconductor lasers with weak, dispersive optical feedback. *Optics letters*, 19(17):1331–1333, 1994.
- [53] Marin Soljačić and John D Joannopoulos. Enhancement of nonlinear effects using photonic crystals. *Nature materials*, 3(4):211–219, 2004.
- [54] Kerry J Vahala. Optical microcavities. *nature*, 424(6950):839–846, 2003.
- [55] Chia Wei Hsu, Bo Zhen, Jeongwon Lee, Song-Liang Chua, Steven G Johnson, John D Joannopoulos, and Marin Soljačić. Observation of trapped light within the radiation continuum. *Nature*, 499(7457):188–191, 2013.
- [56] Chia Wei Hsu, Bo Zhen, A Douglas Stone, John D Joannopoulos, and Marin Soljačić. Bound states in the continuum. *Nature Reviews Materials*, 1(9):1–13, 2016.
- [57] Mikhail F Limonov, Mikhail V Rybin, Alexander N Poddubny, and Yuri S Kivshar. Fano resonances in photonics. *Nature Photonics*, 11(9):543–554, 2017.
- [58] Eric D Black. An introduction to pound–drever–hall laser frequency stabilization. *American journal of physics*, 69(1):79–87, 2001.
- [59] Anton Frisk Kockum, Adam Miranowicz, Simone De Liberato, Salvatore Savasta, and Franco Nori. Ultrastrong coupling between light and matter. *Nature Reviews Physics*, 1(1):19–40, 2019.
- [60] P Forn-Díaz, L Lamata, E Rico, J Kono, and E Solano. Ultrastrong coupling regimes of light-matter interaction. *Reviews of Modern Physics*, 91(2):025005, 2019.
- [61] Philip Krantz, Morten Kjaergaard, Fei Yan, Terry P Orlando, Simon Gustavsson, and William D Oliver. A quantum engineer’s guide to superconducting qubits. *Applied Physics Reviews*, 6(2):021318, 2019.
- [62] Ondřej Černotík, Aurélien Dantan, and Claudiu Genes. Cavity quantum electrodynamics with frequency-dependent reflectors. *Physical review letters*, 122(24):243601, 2019.
- [63] Howard J Carmichael. *Statistical methods in quantum optics 2: Non-classical fields*. Springer Science & Business Media, 2009.
- [64] Yoshihisa Yamamoto and Atac Imamoglu. Mesoscopic quantum optics. *Mesoscopic Quantum Optics*, 1999.
- [65] Weng W Chow, Stephan W Koch, and Murray III Sargent. *Semiconductor-laser physics*. Springer Science & Business Media, 2012.

- [66] Hermann Haken. *Waves, photons, atoms*, volume 1. North Holland, 1981.
- [67] Naturally, in the sense that second-order nonlinearities “naturally” produce squeezed states.
- [68] By “non-perturbative”, we mean that the resulting intensity-dependent loss cannot be approximated by a low-order Taylor expansion about zero intensity.
- [69] In either case, we will refer to the dissipation as absorption. Even in the case of radiative leakage, the cavity photon can be seen as being absorbed by the beam of far-field radiation exiting the cavity.
- [70] States for which  $(\Delta n)^2 < \langle n \rangle$ , referred to as sub-Poissonian states, are intrinsically non-classical, and the degree of non-classicality of such states is typically quantified by the Fano factor  $F = (\Delta n)^2 / \langle n \rangle$ .
- [71] While not the focus of our paper, we point out that more general nonlinear loss profiles in principle allow more arbitrary sharpening of the quantum statistics of light, allowing realization of various super-Poissonian, bimodal, and other types of photon probability distributions, which may have applications in probabilistic computing
- [72] This is insofar as the adiabatic approximation is respected, see SI.
- [73] An exact record for the most sub-Poissonian macroscopic state of light is not completely clear from the literature. An upper bound of 50% is provided by works on sub-Poissonian lasers (discussed in Section IV.), however that bound was likely not reached.
- [74] The effects of two-photon absorption (TPA) are not considered here. Estimates for materials such as GaP with similar  $n_2$  indicate that TPA losses are of the same order of magnitude as the losses presented in Fig. 5(b). This can be mitigated by working for example with a different gain medium (with a lasing transition below the half-gap at 1100 nm), or changing the detuning of the cavity from the transmission feature, or working further away from the minimum of the loss curve in panel (b). In this example, we are mainly aiming to be illustrative, showing that typical nonlinear scales and cavity parameters allow this effect to be in principle realized.